

# Dalton Transactions

Accepted Manuscript



This is an *Accepted Manuscript*, which has been through the Royal Society of Chemistry peer review process and has been accepted for publication.

*Accepted Manuscripts* are published online shortly after acceptance, before technical editing, formatting and proof reading. Using this free service, authors can make their results available to the community, in citable form, before we publish the edited article. We will replace this *Accepted Manuscript* with the edited and formatted *Advance Article* as soon as it is available.

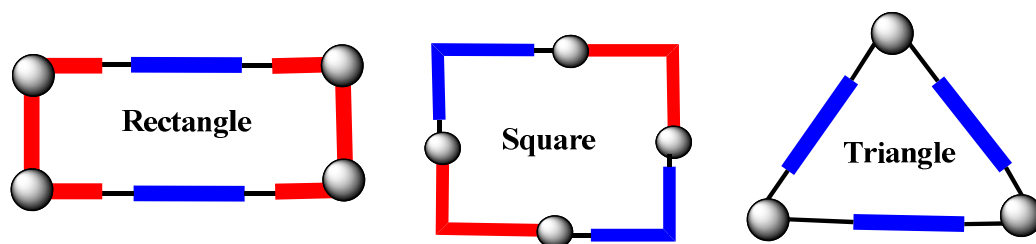
You can find more information about *Accepted Manuscripts* in the [Information for Authors](#).

Please note that technical editing may introduce minor changes to the text and/or graphics, which may alter content. The journal's standard [Terms & Conditions](#) and the [Ethical guidelines](#) still apply. In no event shall the Royal Society of Chemistry be held responsible for any errors or omissions in this *Accepted Manuscript* or any consequences arising from the use of any information it contains.

**Manuscript ID: DT – PER – 01 – 2014 – 000277**

**Title: Supramolecular Architectures with Pyridine-amide Based Ligands: Discrete Molecular Assemblies and Their Applications**

**Graphical Abstract**



This perspective offers an overview on the recent progress achieved in the design of discrete molecular assemblies utilizing assorted pyridine-amide based ligands.

## Supramolecular Architectures with Pyridine-amide Based Ligands: Discrete Molecular Assemblies and Their Applications

Anurag Mishra<sup>1,\*</sup> and Rajeev Gupta<sup>2,\*</sup>

<sup>1</sup>Department of Chemistry, Indian Institute of Technology – Kanpur,  
Kanpur – 208016, India

<sup>2</sup>Department of Chemistry, University of Delhi, Delhi – 110 007, India

### Abstract.

Recent years have seen a surge of interest in supramolecular architectures with focus shifting towards generating discrete molecular assemblies and factors controlling their formation. Such molecular assemblies offer wide range of applications which are often architecture-dependent. To construct such assemblies, nitrogen-donor ligands have been intensively employed to generate an assorted variety of topologies. Out of various nitrogen-donor ligands; pyridine-amide based ligands stand out as they not only offer structural flexibility and their ability to adjust to the geometrical requirements of a metal ion but also offer dual functional groups; pyridine and amide. The present perspective will focus on recent developments in the design of discrete supramolecular assemblies utilizing pyridine-amide based ligands with a specific stress on the architectural aspects and subsequent applications of designed molecular assemblies.

## 1. Introduction.

The development of supramolecular chemistry in the last two decades has added a whole new perspective to modern chemistry by applying non-covalent interactions in a rational way to organize molecular components and thus justifying the concept of “chemistry beyond the molecule”.<sup>1,2</sup> It has been amply demonstrated that the non-covalent interactions offer incredible opportunity for the synthesis of large and complex structures with applications as assemblies, receptors, and devices.<sup>3</sup> The concepts of supramolecular chemistry have also been extended to other established fields, such as polymer science,<sup>4</sup> solid-state chemistry,<sup>5</sup> and liquid-crystal research.<sup>6</sup> In general, the construction of highly complex system is apparently not feasible by means of a singular non-covalent interaction; rather, a manifold of interactions of converging strength, directionality, and complementarity have to be applied and balanced to achieve the structure formation over multiple levels with the assembly process gradually increasing in strength.<sup>7,8</sup> In this context, designed multidentate ligands with assorted functionalities are of utmost importance. Pyridine-amide based ligands have always attracted the scientific community to explore their metallo-supramolecular chemistry. This is primarily due to the dual ability of such ligands to self-assemble through coordination bond formation (*via* pyridine) in conjunction with hydrogen bonding (*via* amide C=O and N-H groups) capabilities.

Metal-ligand coordination provides an excellent means for the synthesis of metallo-supramolecular systems as (i) a coordination bond is highly directional; (ii) the ligand structure can be varied in a desirable manner by established synthetic chemistry; and (iii) the thermodynamic and kinetic stability can be fine-tuned with the appropriate selection of ligand type(s) and metal ion(s).<sup>9-11</sup> Supramolecular systems constructed from the metal–ligand bonds include chains, layers, sheets, cyclic, and filamentous as well as interlaced systems.<sup>12-14</sup>

In recent times, various methodologies for the rational design of multi-dimensional structures have been developed, led by the groups of Stang,<sup>15-17</sup> Raymond,<sup>18-20</sup> Fujita,<sup>21-23</sup> Therrien,<sup>24-26</sup> and Puddephatt<sup>27-29</sup> and adequately followed by others.<sup>30-39</sup> This rational design strategy allows for a combinatorial molecular library consisting of complementary molecular components that allows one to think retro-synthetically on how best to achieve the geometry of a particular discrete assembly. A large number of intriguing molecular assemblies, such as molecular triangles, squares, rectangles, cages, and metallacycles have been synthesized using pyridine-amide based ligands and suitable metal ions. Therefore, metallo-supramolecular architectures *via* coordination-driven self-assembly is at the forefront of supramolecular chemistry and will continue to attract focused research.

## 2. Scope of the Review.

The purpose of the present review is to cover recent developments in the area of supramolecular coordination chemistry with pyridine-amide based ligands. The emphasis has been given to delineate the synthetic strategies towards potentially tailor-made self-assembled architectures. As much as possible, in addition to the structural discussion, functional aspects of the resultant architectures are included. It is important to mention that the supramolecular coordination chemistry has grown significantly and a number of comprehensive reviews detailing design, structure, and applications are available in the literature. However, a focused discussion on the self-assembly aspects of pyridine-amide based ligands has not been attempted despite notable examples and tremendous expansion possibilities. Therefore, this review does not attempt to exhaustively present all known supramolecular coordination complexes, which would require extensive page lengths and many references, thus limiting its practical significance. Instead, representative examples are collected in each section highlighting the relationship between the

geometrical parameters offered by a particular class of pyridine-amide based ligands and metal ions/complexes to encompass pioneering work to contemporary discoveries. The reader will also be directed to a number of relevant papers and reviews, which will arouse further investigations into a particular aspect of metallo-supramolecular chemistry.

### 3. Design Strategies.

A coordination bond between a metal center and a suitable organic ligand is the fundamental requirement for the construction of a coordination-driven supramolecular structure. Whether the resultant structure would be a discrete complex, a large complex, a supramolecular complex, or a network depends on several parameters encompassing both ligand and metal based starting materials. An important prerequisite is the geometrical and/or directional control over the approach between the ligand(s) and a metal ion. Supramolecular coordination complexes are discrete constructs, typically obtained by mixing suitable metal and ligand precursors that spontaneously form metal–ligand bonds to generate a single thermodynamically favored product. Typically, the metal ions are introduced into these structures with directing or blocking ligands that only make coordination sites available to incoming ligands with appropriate angle to form the desired shape. One of the greatest advantages offered by this approach is the possibility to predetermine the shape and size of the target molecule by careful selection of the metal-based starting material, coordinatively inert directing ligands, and rigid bridging ligands. Figure 1 illustrates the common design strategies employed for the construction of discrete supramolecular architectures. For example, combination of a metal-based clip together with two rigid linear linkers of differing lengths in the absence of any driving bias should result in a molecular rectangle (Figure 1a). Similarly, a molecular square can be achieved via self-assembly of angular and linear units in two complementary ways: (i) by using a metal starting material

with a  $90^\circ$  angle between the coordination sites and a rigid linear ligand; or (ii) by utilizing both metal complex as well as ligand system with a  $90^\circ$  turn (Figures 1b and 1c, respectively). A molecular triangle can be prepared by the combination of three bent donor units ( $60^\circ$ ) and three linear ( $180^\circ$ ) acceptors (Figure 1d). In a similar manner, a dinuclear metallacycle can be assembled by using a metal complex with a  $60^\circ$  angle between the coordinately labile sites and a rigid ligand/linker with a  $120^\circ$  angle (Figure 1e). The combination of three bidentate bent linking units with two tridentate angular components will result in a molecular cage (Figure 1f). One can utilize these design strategies as a reference point and plan assorted organic ligands and metal-based starting materials fulfilling the geometrical requirements as the potential molecular components towards aesthetic yet functional architectures.

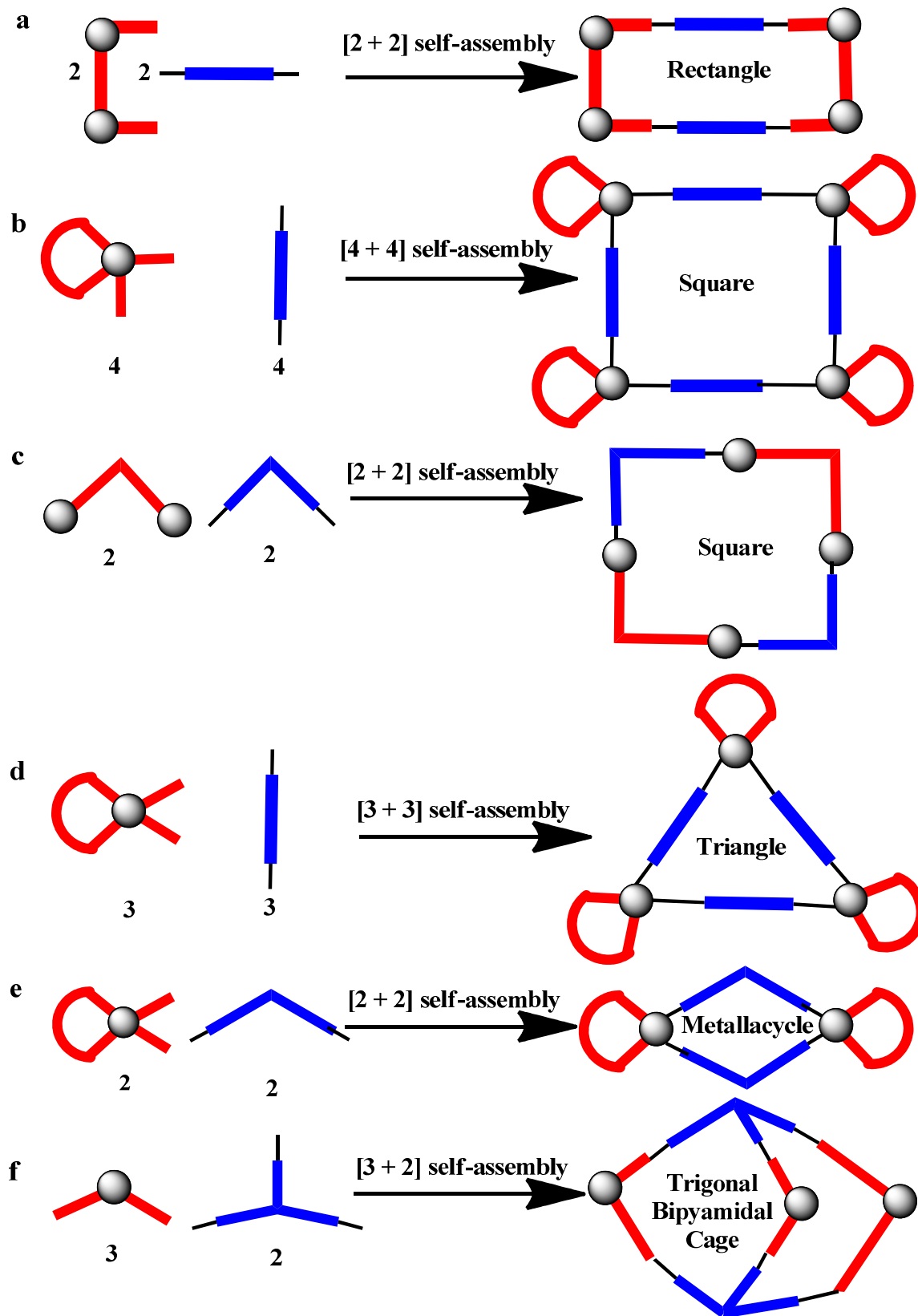


**Fig. 1** Schematic representations of the self-assembly of various molecular components

#### 4. Why Pyridine-amide Based Ligands?

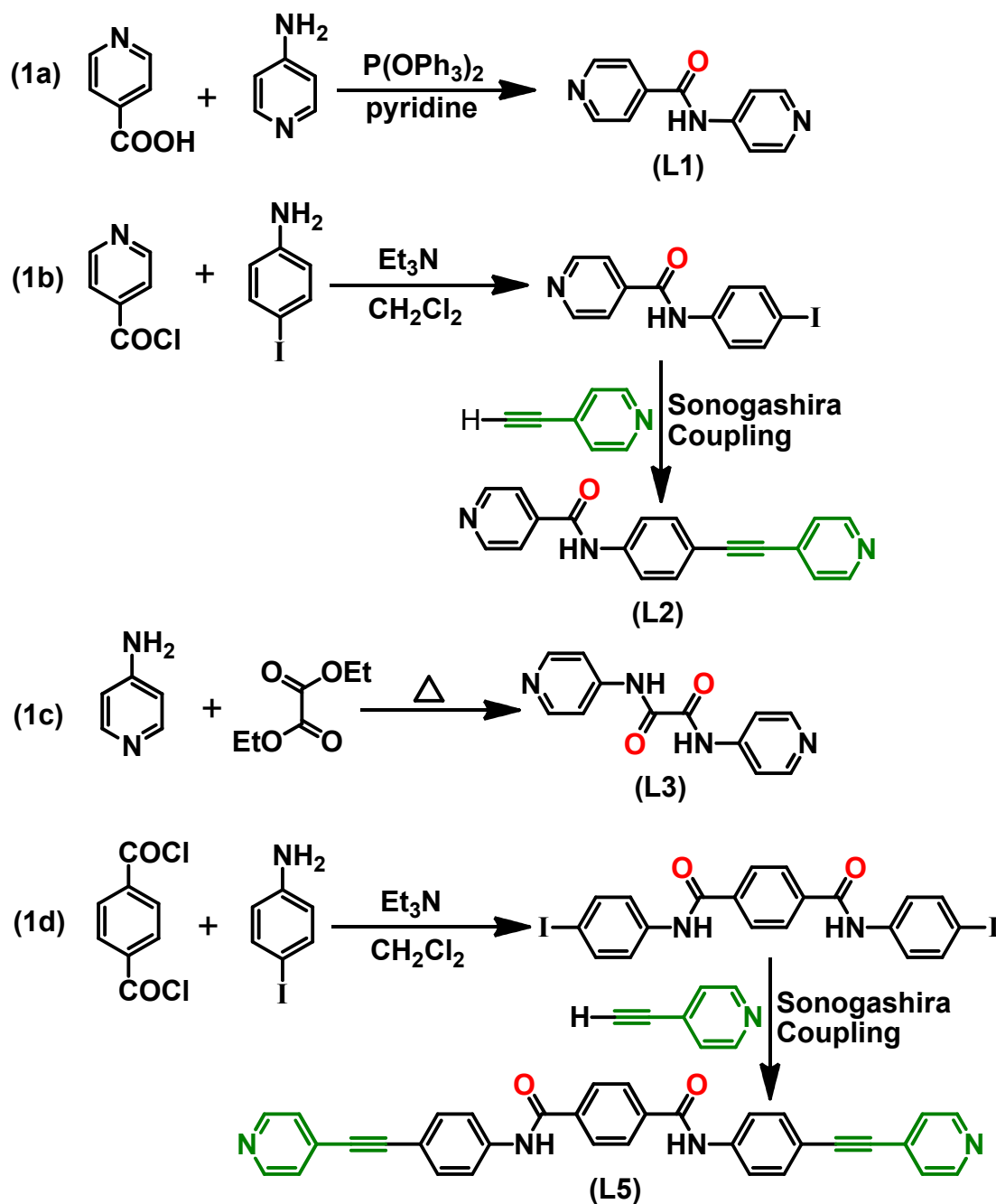
As discussed in the previous section, geometrical aspects originating from the organic ligand as well as metal precursor primarily control the synthetic outcome of the resultant supramolecular architecture. In addition, secondary parameters such as choice of the metal salt and solvent(s), reaction conditions including temperature, and even stoichiometry tend to influence the end result. A metal precursor is likely to be geometrically rigid; therefore, the associated organic ligand should offer structural flexibility for a viable organization to the resultant supramolecular architecture. Out of several classes of organic ligands; pyridine-amide based ligands not only offer structural flexibility and their ability to adjust to the geometrical requirements essential for the construction of a supramolecular architecture but also offer coordinating functional groups (*i.e.* pyridine). The structural flexibility originates from the facile rotation of functional groups attached to an amide group,  $-\text{CONH}-$ . Interestingly, such a structural flexibility allows the possibility of several geometrical isomers of an amide-based ligand and thus provides another architectural parameter. The appended pyridine functional groups could be connected at several positions (2-pyridyl, 3-pyridyl, or 4-pyridyl) thus expanding their coordination versatility. Finally, presence of hydrogen bonding synthons (*via* amide C=O and N-H groups) opens up the binding and/or sensing possibilities. A suitable combination of such parameters generates a range of interesting ligands with assorted architectural possibilities and applications.

#### 5. Assorted pyridine-amide ligands; general synthetic methodologies.

This perspective has discussed a variety of pyridine-amide based ligands which have been designed to provide degrees of flexibility and orientation of the pyridyl donor group(s) while retaining the amide group(s) that can take part in hydrogen bonding. Although, such ligands can be synthesized in several ways;<sup>30a</sup> a few preparative routes have been included here for the

benefit of the readers. It is anticipated that other multidentate ligands could also be envisioned via a similar synthetic methodology available in the literature.

The ligand **L1** was synthesized by coupling 4-aminopyridine with isonicotinic acid in pyridine in presence of  $P(\text{OPh})_3$  as the coupling agent (Scheme 1a).<sup>30a,32</sup> Alternatively, 4-aminopyridine can be coupled with isonicotinoyl chloride in the presence of  $\text{Et}_3\text{N}$  in a suitable solvent such as  $\text{CH}_2\text{Cl}_2$ . The ligand **L2** was synthesized in two steps.<sup>33,34</sup> In the first step, the precursor (4-iodophenyl)pyridine-carboxamide, was prepared by coupling 4-iodoaniline with isonicotinoyl chloride in  $\text{CH}_2\text{Cl}_2$  in the presence of  $\text{Et}_3\text{N}$ . In the second step, Sonogashira coupling of (4-iodophenyl)pyridine-carboxamide was carried out with 4-ethynylpyridine in DMF (Scheme 1b). Notably, ligand **L2** is an extended version of ligand **L1** by the incorporation of phenylethynyl fragment which not only increases the spacer length between two pyridine rings but also assimilates an electron deficient moiety in the resultant assembly. Such structural features strongly influence the outcome of the resultant material. The ligand **L3** was synthesized in a single step by treating 4-aminopyridine with diethyl oxalate (Scheme 1c).<sup>35</sup> This ligand provides two symmetrical fragments of 4-pyridinecarboxamide on either side while potentially offering two sets of H-bonds donors and acceptors. The ligand **L5** was synthesized in two steps.<sup>37</sup> Initially, precursor  $N,N'$ -bis(4-iodophenyl)terephthalamide was obtained by coupling 4-iodoaniline and terephthaloyl dichloride in  $\text{CH}_2\text{Cl}_2$  in presence of  $\text{Et}_3\text{N}$ . The resulting product was then coupled with 4-ethynylpyridine in DMF under standard Sonogashira coupling conditions to afford the final ligand **L5** (Scheme 1d). Interestingly, **L5** is a much extended ligand that also incorporates two electron-deficient alkyne moieties thus suggesting potential sensing applications.



Scheme 1. Preparative routes for the synthesis of a few representative ligands.

The next few sections have collected intriguing examples where assorted pyridine-amide based ligands have been used for the construction of discrete supramolecular assemblies. In all such examples, the pyridine-amide based ligands have adjusted to the geometrical requirements

and adapted various conformations that have allowed the stabilization and construction of an interesting discrete architecture.

## 6. Two dimensional structures

### 6.1 Molecular Rectangles

The coordination bonding motif of pyridyl-based ligands with metal acceptors has proven very useful for the construction of a wide variety of molecular shapes including rectangles. However, despite relative topological simplicity; the synthesis of molecular rectangle is not straightforward. Geometrically, combination of a 90° metal acceptor with two rigid linear linkers of differing lengths in the absence of any driving bias should result in a molecular rectangle.<sup>31-43</sup> Various research groups have developed different synthetic strategies for the preparation of supramolecular rectangles with assorted pyridine-amide donors. Mukherjee and coworkers<sup>31</sup> have displayed a [2 + 2] self-assembly of a diplatinum(II) molecular clip **A1** with a linear asymmetrical bis(pyridyl) ligand, **L1**, towards the formation of a symmetrical rectangle **1** (Figure 2). Out of two possible linkage isomers, only the most symmetrical one was synthetically observed on the basis of multinuclear NMR, mass spectrometry, and X-ray diffraction studies. The solid-state crystal structure of tetra-cationic rectangle **1** shows that the bis(pyridyl) ligands occupy the long edges of the rectangle.

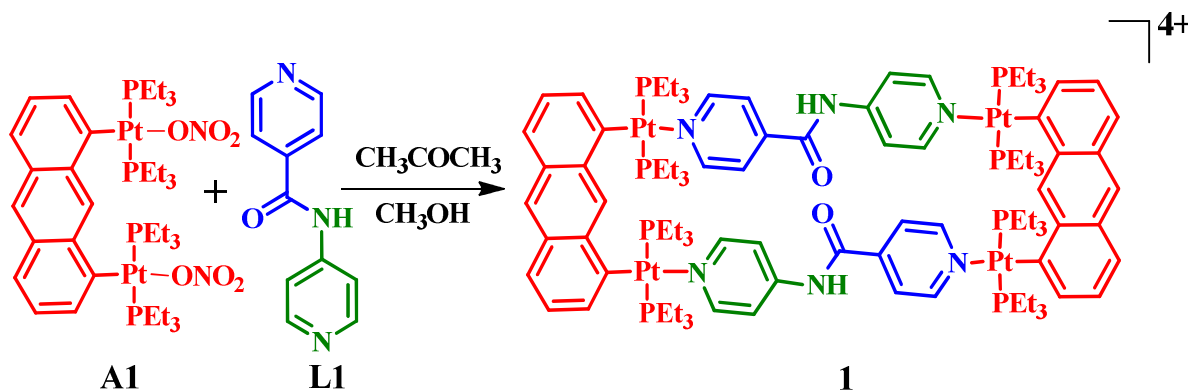


Fig. 2 Pt based molecular rectangle; adapted from ref. 31.

The tetra-cationic molecular rectangles **2** and **3** were prepared by the coordination-driven self-assembly of half-sandwich *p*-cymene-capped Ru(II)-based binuclear “clip” acceptors **A2** or **A3** with a flexible bidentate amide linker **L1** in 1:1 molar ratio (Figure 2).<sup>32</sup> These molecular rectangles were characterized by multinuclear NMR, IR, and ESI-MS spectroscopic studies as well as single-crystal X-ray diffraction studies. The molecular structures of **2** and **3** adapt a similar tetranuclear rectangular geometry composed of  $[(p\text{-cymene})_4\text{Ru}_4(\mu\text{-}\eta^4\text{-oxalato})_2(\text{L1})_2]^{4+}$  (**2**) and  $[(p\text{-cymene})_4\text{Ru}_4(\mu\text{-}\eta^4\text{-quinonato})_2(\text{L1})_2]^{4+}$  (**3**). Each Ru center is coordinated to one nitrogen atom of the **L1** linker and two oxygen atoms from the oxalato (**2**) or quinonato (**3**) moieties resulting in a tetranuclear rectangular assembly with the dimensions of 5.51 Å × 13.29 Å for **2** and 7.91 Å × 13.46 Å for **3**. Interestingly, despite the fact that amide linker **L1** binds to the Ru centers in a head-to-tail fashion in both rectangles; the structures were quite different with respect to the orientation of the amide groups. The carbonyl moieties of the amide groups were directed parallel in **2** but antiparallel in **3** (Figure 3).

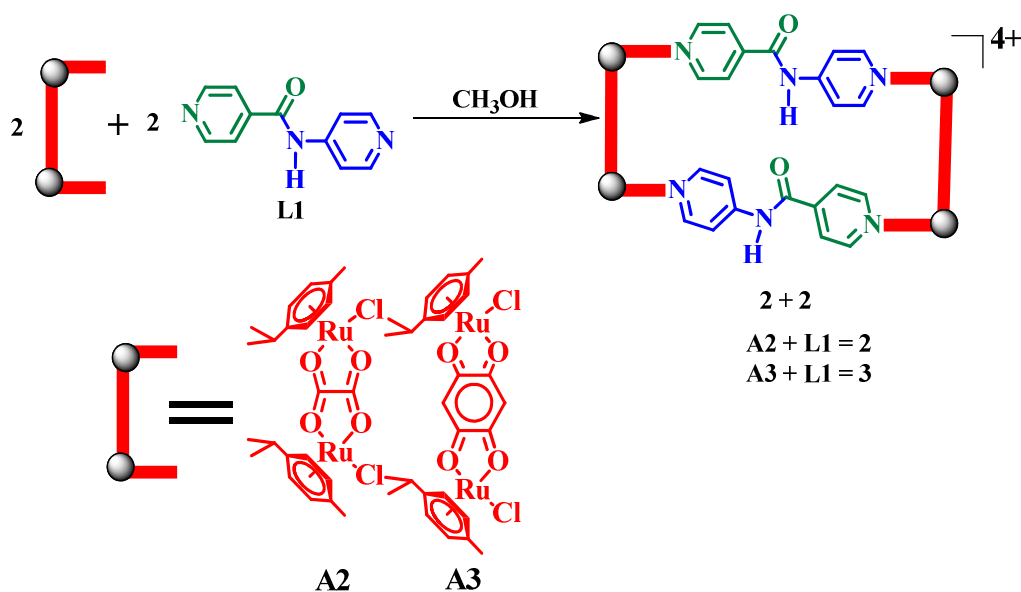
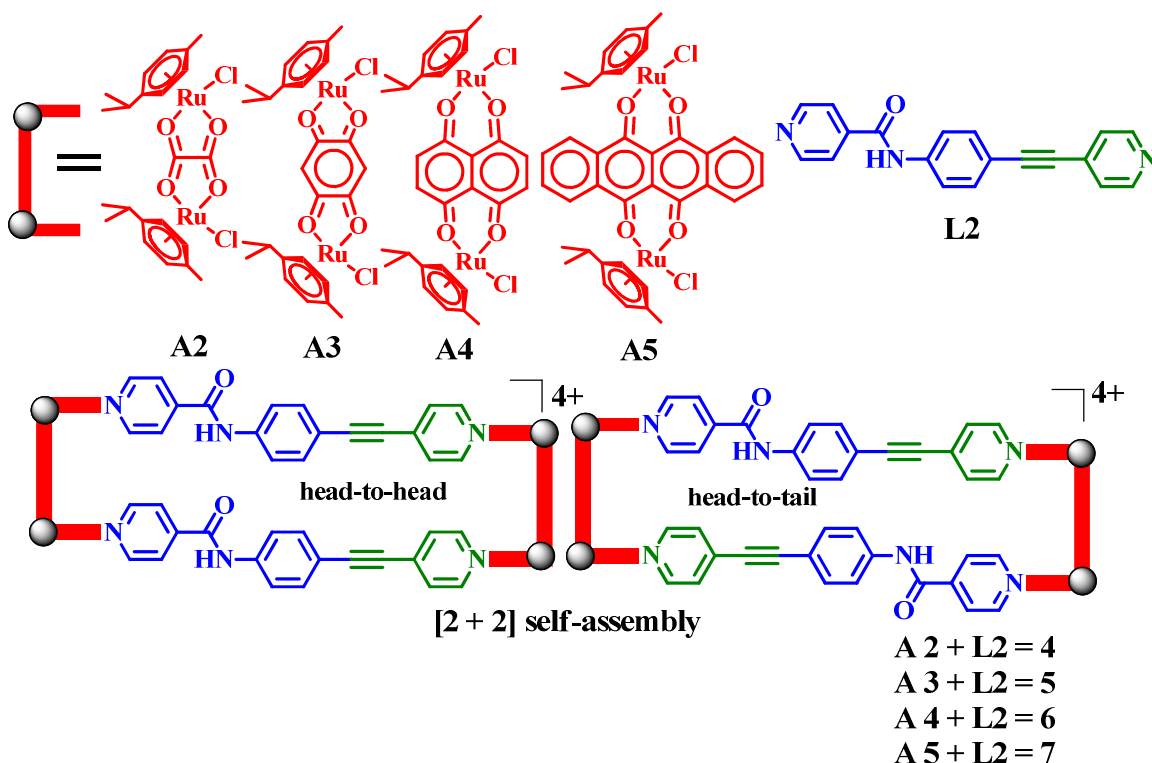


Fig. 3 Ru based molecular rectangles; adapted from ref. 32.

Chi and coworkers have reported various ruthenium based molecular rectangles using assorted arene-ruthenium acceptors and amide-based ligands (Figure 4).<sup>33-39</sup> When arene-ruthenium acceptors, **A2-A5**, and an unsymmetrical pyridyl-ethnyl-amide ligand **L2** were used in the self-assembly; two isomeric products were obtained (Figure 4).<sup>33,34</sup> Due to unsymmetrical nature of ligand **L2**, a 1:1 mixture of two structural isomers, *head-to-tail* and *head-to-head* were obtained. X-ray crystallography unambiguously established the rectangular shape of products **4** and **7**. The structural analysis of **4** revealed that the two pyridyl moieties bridge with two  $[(Ru_2(\mu-\eta_4-C_2O_4)(\eta_6-p-Pr^iC_6H_4Me)_2)]^{4+}$  units to form an  $M_4L_2$  rectangle. Interestingly, despite head-to-tail binding of ligand **L2** to the Ru centers, the amidic C=O and NH moieties were aligned in opposite direction. The self-assembled rectangles **4** and **6** were further screened for *in-vitro* anticancer activities where **A4** containing rectangle **6** was found to be considerably effective against several cancer cell lines.<sup>33</sup> The naphthacenedione containing rectangle **7** was used for anion sensing with the amide linkages serving as the hydrogen bond (H-bond) donor sites for anion and the ruthenium moiety serving as the signaling unit.<sup>34</sup> The UV/Vis titration study demonstrated that rectangle **7** interacts weakly with common mono-anions as well as with flexible dicarboxylate anions such as malonate and succinate. Notably however, rectangle **7** showed significant affinity for rigid multi-carboxylate anions such as oxalate, citrate, and tartrate. The results suggest that 1:1 hydrogen bonding (H-bonding) assisted by appropriate geometrical complementarity was largely responsible for the enhanced affinity towards such anions. The fluorescence titration showed large fluorescence enhancement upon binding to multi-carboxylate anions. Such a fact could be attributed to the blocking of photo-induced electron-transfer from the arene-Ru moiety to the amidic donor in rectangle as a result of H-bonding between the donor and guest anion.



**Fig. 4** Ru based molecular rectangles; adapted from ref. 33 and 34.

Chi and coworkers have recently reported the synthesis and characterization of two arene-Ru-based rectangles **8** and **9** via [2 + 2] assembly of arene-Ru clips **A3** and **A5** with diamide-dipyridyl ligand **L3** (Figure 5).<sup>35</sup> Both rectangles were characterized by the various spectroscopic methods. The single crystal X-ray diffraction study of **9** supported the rectangular shape of the self-assembled structure with cavity dimension of  $12.3 \times 6.6 \text{ \AA}^2$ . Notably, a diethyl ether molecule was encapsulated inside the rectangular molecular cavity. The Ru...Ru diagonal length of the rectangular structure **9** was ca.  $15.76 \text{ \AA}$  while the Ru...Ru distance in the dimetallic pillar was  $8.43 \text{ \AA}$ . The centroids of two amidic donors were separated by a distance of  $7.28 \text{ \AA}$ . The diamide moieties on linear ditopic ligands contained H-bonding sites and therefore suggested anion-sensing possibilities.

The naphthacenedione-containing rectangle **9** was used for anion sensing with the amidic linkage serving as the H-bond donor site for anions and the ruthenium moiety functioning as the

signaling unit. A UV/Vis titration study demonstrated that the rectangle interacted weakly with common monoanions and flexible dicarboxylate anions, such as malonate and succinate, but had significant binding affinity for rigid multi-carboxylate anions, such as oxalate, citrate, and tartrate. Oxalate binding was further probed by the Job's plot and analyzing the Stern-Volmer kinetics as well as UV-vis titration which indicated 1:1 binding between receptor **9** and oxalate anion with the binding constant of  $4 \times 10^3 \text{ M}^{-1}$ . Stern-Volmer constant of  $5 \times 10^4 \text{ M}^{-1}$  was calculated from the photoluminescence titration.

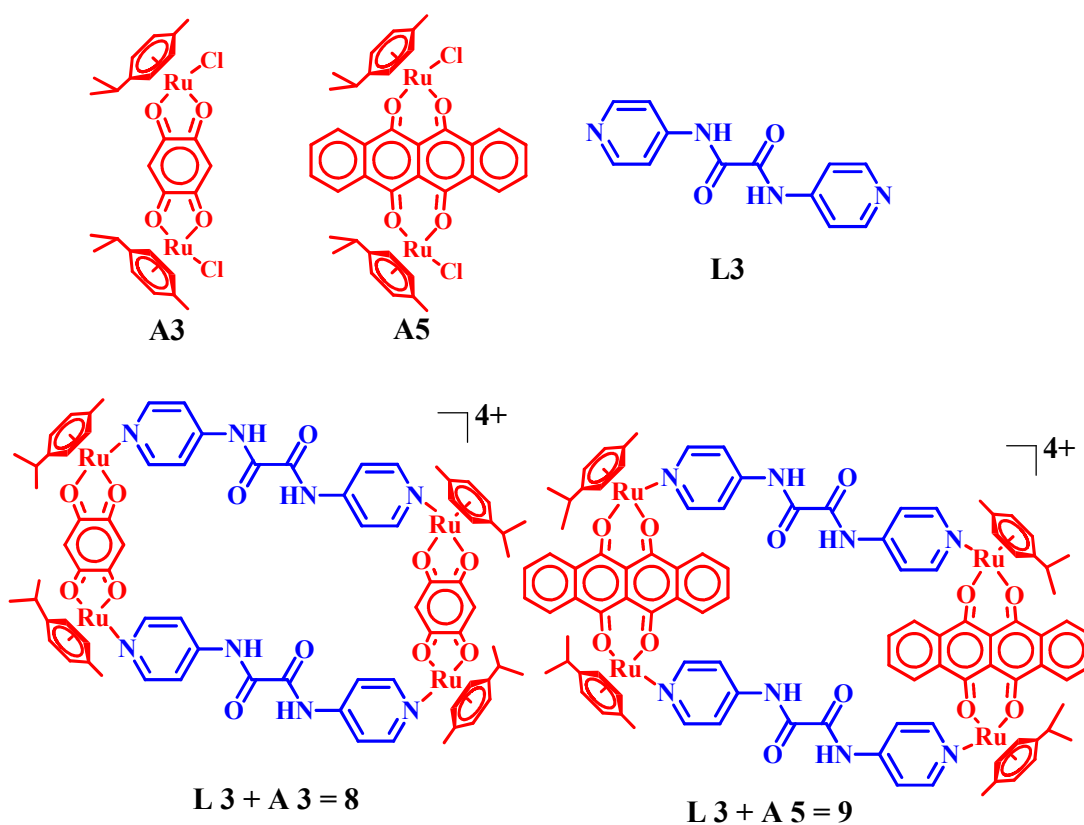


**Fig. 5** Ru based molecular rectangles; adapted from ref. 35.

These authors further reported three tetranuclear molecular rectangles **10-12** that were prepared by the reaction of arene-Ru acceptors **A2** and **A4** with the dipyrindyl-diamide ligands **L3** and **L4** in a 1:1 mixture of nitromethane and methanol (Figure 6).<sup>36</sup> These molecular rectangles were characterized by  $^1\text{H}$  NMR spectroscopy and ESI-MS; while the crystal structures for **10** and

**11** were established by the X-ray diffraction studies. Each ruthenium atom was coordinated by one nitrogen atom of dipyridyl-diamide ligand and two oxygen atoms of oxalato or naphthaquinonato ligand, resulting into the tetranuclear rectangular structures. These self-assembled complexes were tested for *in-vitro* anticancer activity against SK-hep-1 and HCT-15 cancer cell lines. The results displayed that the cytotoxicity of rectangle **12** was comparable or even better than that of reference drug cisplatin.

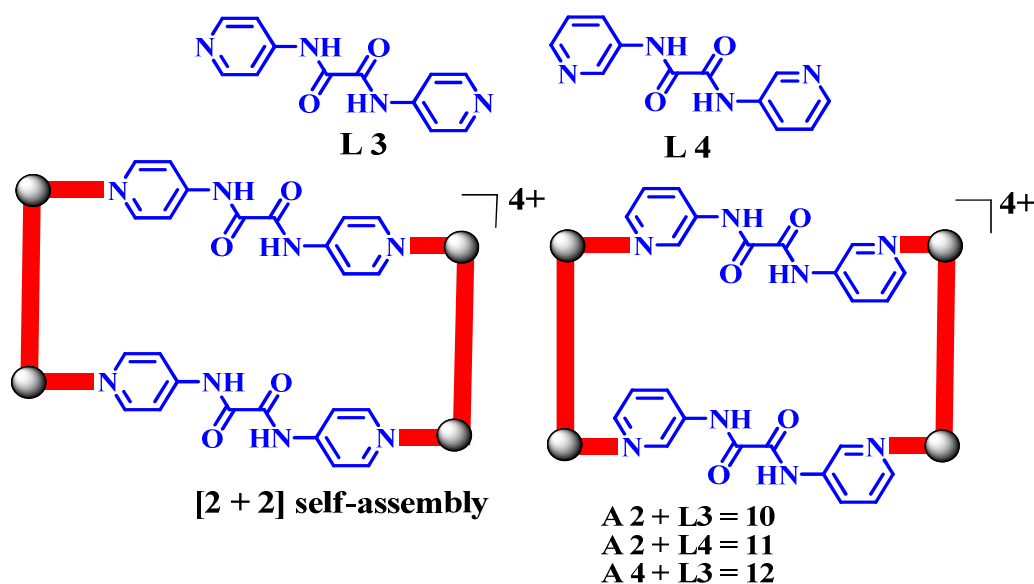


**Fig. 6** Ru based molecular rectangles; adapted from ref. 36.

Very recently, Chi and co-workers have displayed two large molecular rectangles **13** and **14**, from the combination of a symmetrically elongated dipyridyl-diethynyl ligand **L5** centered on a diamide core with two arene-Ru acceptors **A3** and **A5** (Figure 7).<sup>37</sup> These rectangles were characterized by multinuclear NMR, ESI-MS, and UV-Vis spectroscopic studies. The molecular structure of rectangle **13** was unambiguously determined by the single crystal X-ray diffraction analysis as a representative case. The crystal structure of **13** exhibited that two dipyridyl ligands bridge two  $[Ru_2(\text{arene})_2(2,5\text{-dihydroxy-1,4-benzoquinonato})_2]^{4+}$  **A3** units to form a  $[2 + 2]$   $M_4L_2$  rectangle with a large cavity ( $8.5 \times 32.43 \text{ \AA}^2$ ). Due to the presence of an extended  $\pi$ -electron

aromatic surface, the tetracene containing molecular rectangle **14** was capable of binding  $C_{60}$  and  $C_{70}$  fullerenes as quantified by the UV-vis, fluorescence emission and  $^1H$  NMR spectral experiments. These rectangles nicely illustrated example of a supramolecular host capable of recognizing large guest molecules. In addition, conceptual design of such discrete rectangles exhibits a new rationale for the recognition of  $\pi$ -electronic surfaces.

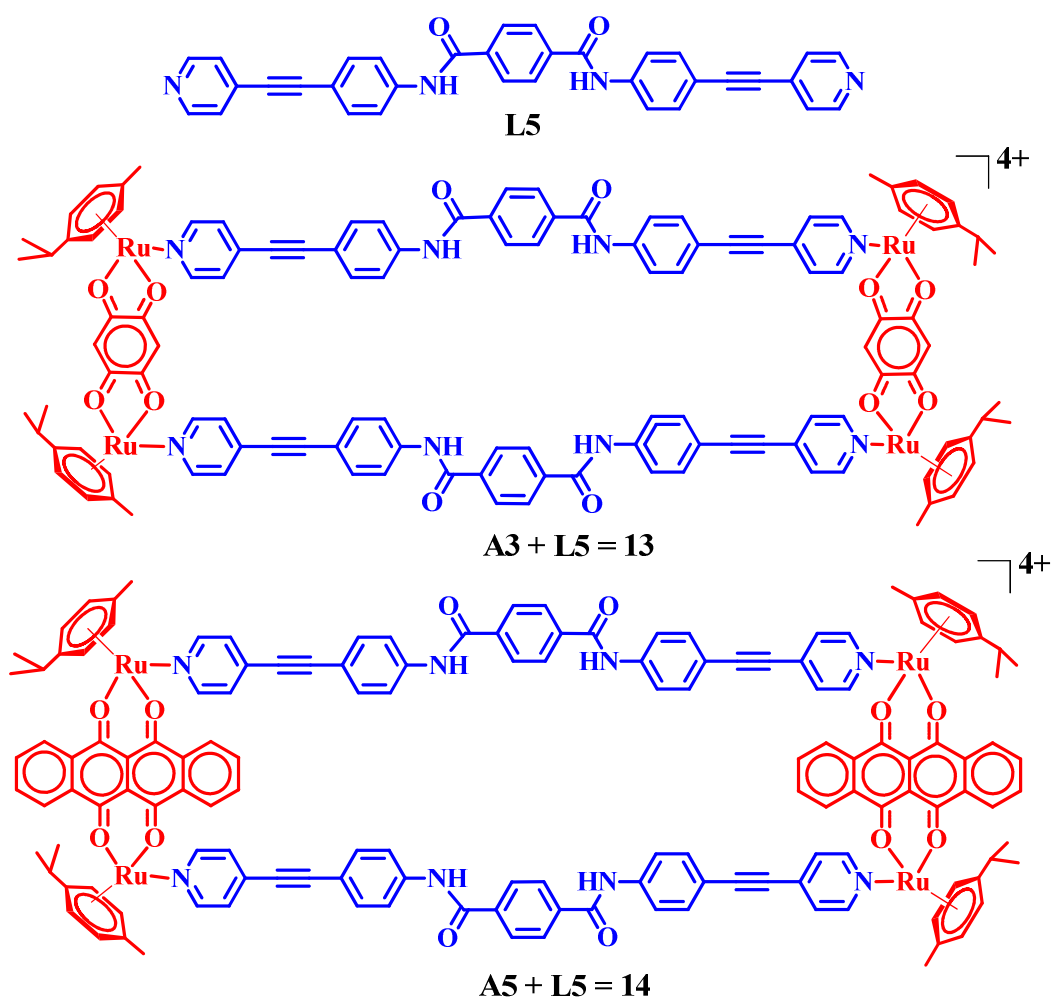


**Fig. 7** Ru based molecular rectangles; adapted from ref. 37.

## 6.2 Molecular Squares

Molecular squares with transition metal corners are equally challenging to construct in synthetic coordination chemistry.<sup>44-48</sup> According to the directional bonding approach; a molecular square

can be constructed by the combination of a 90° corner unit with a linear bridging ligand. Thus, there are two complementary ways to design a molecular square; (i) by the combination of a 90° metal-containing acceptor having two accessible *cis*-coordination sites with linear donor units; and (ii) by using both metal-containing acceptor and ligand with 90° turn. In this context, almost any transition metal with square-planar, trigonal-bipyramidal, or octahedral geometry can be used as a corner unit.

Kitagawa and co-workers<sup>46</sup> have synthesized stacked modes of square-grids which were decorated with the H-bonds and were associated with the dynamic pores. Such a form of H-bond is similar to that of amide bonding of cyclic peptide and is useful for achieving dynamic pores in coordination polymers. The reactions of bis-pyridyl ligands with amide spacer (**L1** and **L6**) with suitable metal salts afforded 2D motifs with deformed square-grid structure;  $[\text{Co}(\text{NO}_3)_2(\text{L1})_2]_n$  (**15**) and  $\{[\text{Co}(\text{NCS})_2(\text{L6})_2] \cdot 4\text{Me}_2\text{CO}\}_n$  (**16**  $\supset$   $4\text{Me}_2\text{CO}$ ) (Figure 8). Notably, 2D molecular squares are bound by complementary H-bonds between the amide groups resulting in the creation of a 3D stacked network. In case of **16**  $\supset$   $4\text{Me}_2\text{CO}$ , the amide groups form a contrivance for a dynamic porous framework because of their relevant position and orientation in the mutual nearest neighboring motifs. Consequently, **16**  $\supset$   $4\text{Me}_2\text{CO}$  shows amorphous (nonporous)-to-crystalline (porous) structural rearrangement in the  $\text{Me}_2\text{CO}$  adsorption and desorption process where the 2D framework structure is maintained.

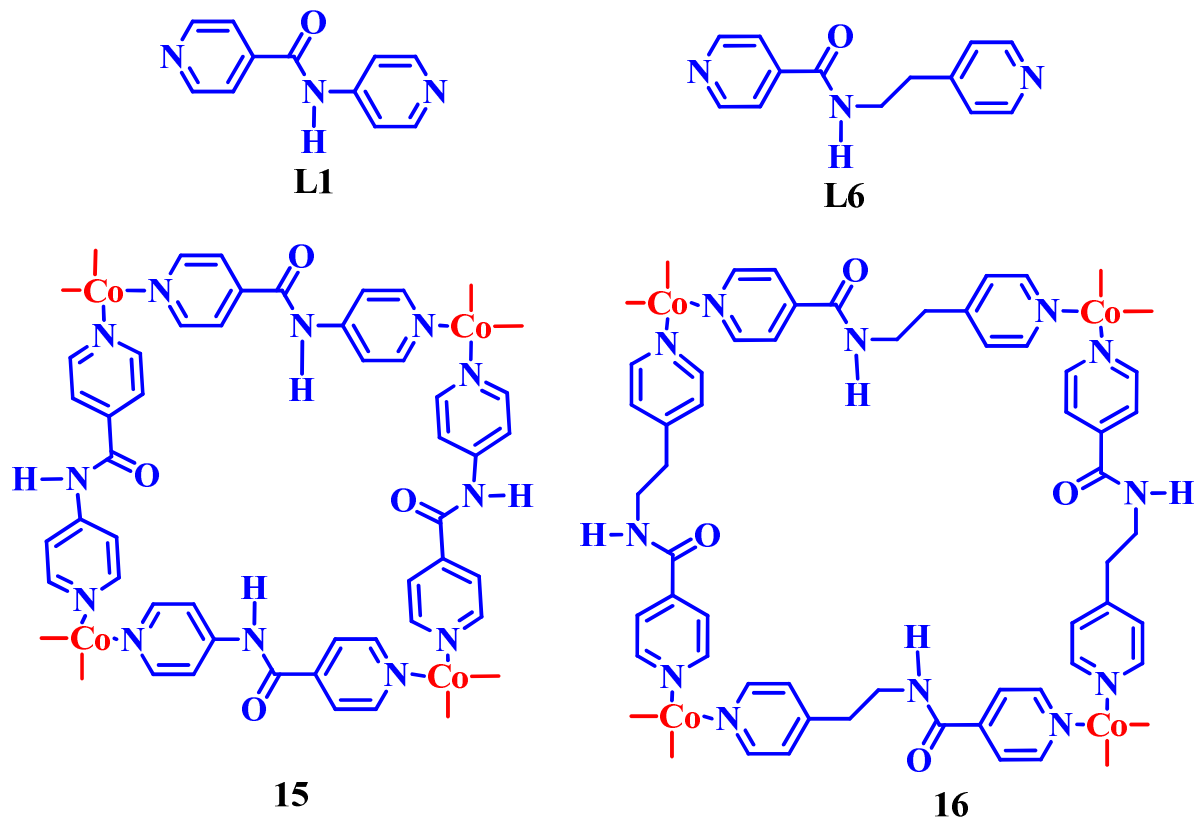


**Fig. 8** Co based molecular squares; adapted from ref. 46.

Tzeng and co-workers<sup>47</sup> have displayed notable anion recognition by a Re(I) based molecular square **17** containing the dipyriddy-amide ligand **L3** (Figure 9). The molecular square,  $[\text{Re}(\text{CO})_3\text{Cl}(\text{L3})]_4$  (**17**), was constructed from  $\text{Re}(\text{CO})_5\text{Cl}$  and **L3**. The anion recognition studies for molecular square **17** showed largest binding constant for a highly electronegative anion,  $\text{F}^-$ , whereas the less electronegative and bigger anions (such as  $\text{Br}^-$ ) displayed poor binding affinity.

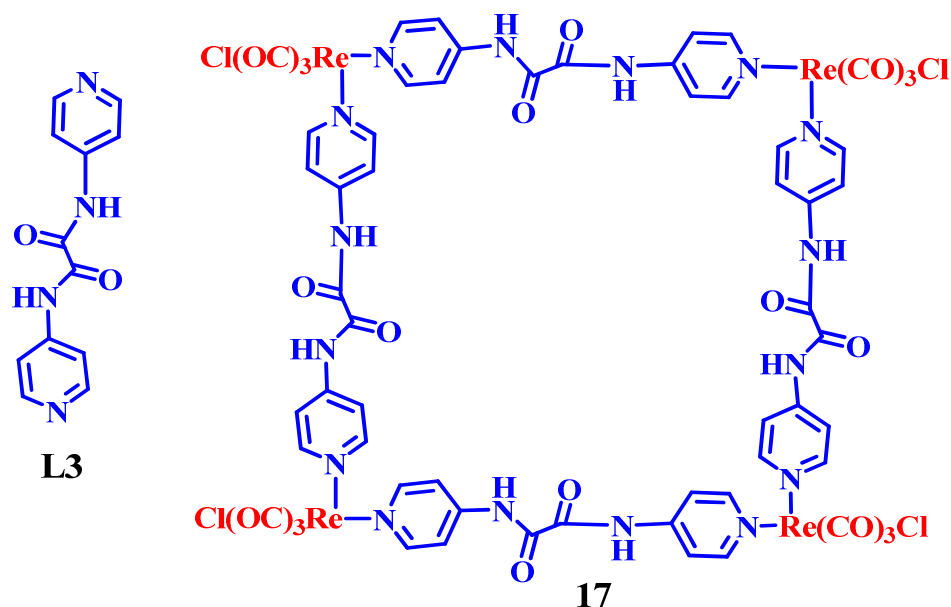


**Fig. 9** Re based molecular square; adapted from ref. 47.

Ballester and co-workers<sup>48</sup> have synthesized a  $\text{M}_2\text{L}_2$  molecular square **18** via combination of a square-planar *cis*-protected  $[\text{Pt}(\text{dppp})(\text{O}_3\text{SCF}_3)_2]$  acceptor **A6** and a ditopic ligand **L7** in a 1:1 ratio at room temperature in  $\text{CDCl}_3$  (Figure 10). The  $\text{M}_2\text{L}_2$  square was characterized by the multinuclear NMR spectroscopy and X-ray diffraction analysis. The X-ray structure confirmed the formation of square-shaped metallacycle **18** in the solid state and revealed the presence of two triflate anions inside the cavity while the other two were positioned at a distance of 3.179 Å from the Pt(II) centers. A careful look to the crystal structure displays the existence of anion... $\pi$  interactions. Such interactions were observed for both triflate anions confined inside the cavity. Moreover, triflate anions that were present inside the cavity of the metallacycle were H-bonded to three water molecules. The existence of chemically non-equivalent triflate anions within as well as outside the cavity was clearly visible by the observation of two separate fluorine signals in the NMR spectra.

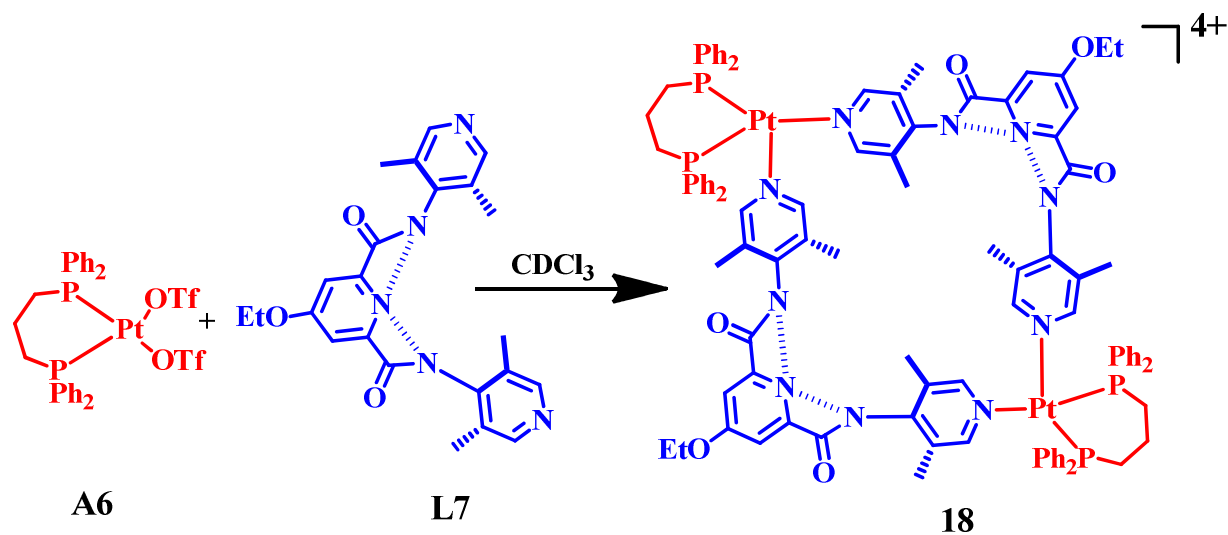
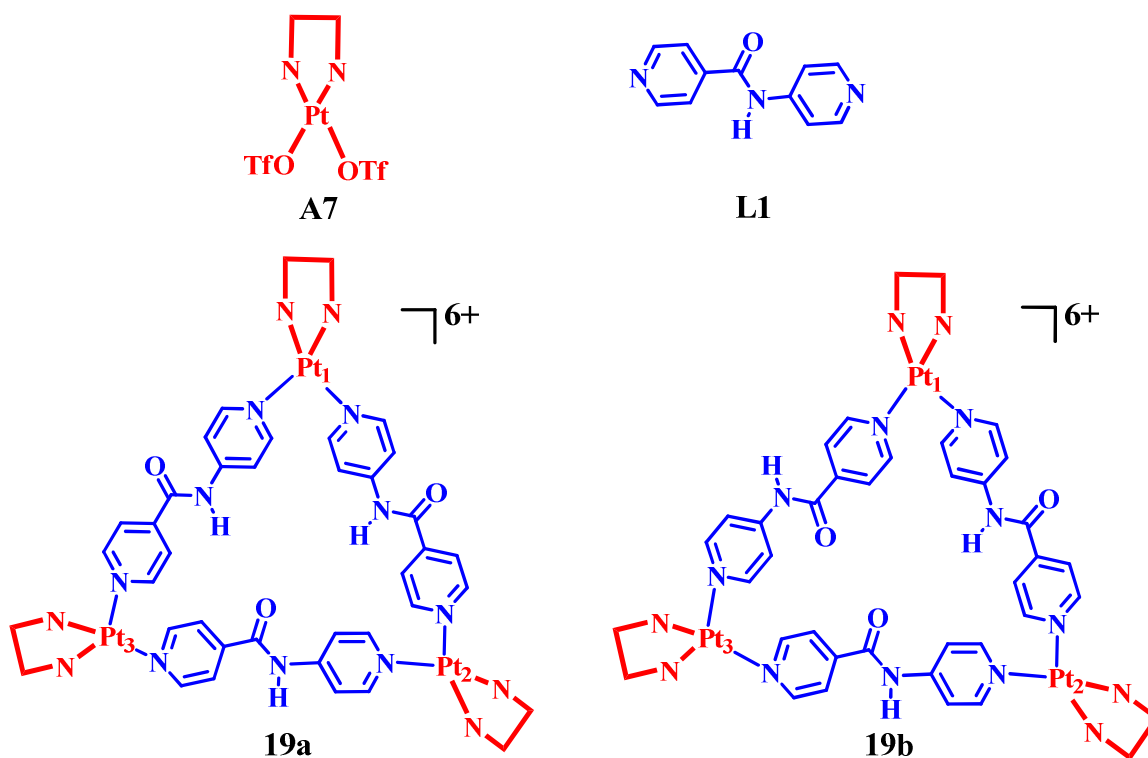


Fig. 10 Pt based molecular square; adapted from ref. 48.

### 6.3 Molecular Triangles

There has been a great interest in metallo-supramolecular chemistry to design molecular triangles assembled through coordination bonds. Notably, some of these triangles were found to stack to generate materials with nanometer sized channels. However, the stacking has usually been unpredictable and therefore the discovery of stacked triangles has often been serendipitous.<sup>49</sup> Puddephatt and co-workers have shown an intriguing example of two Pt<sup>2+</sup>-based triangles by employing unsymmetrical L1 as the bridging ligand and a Pt(II) compound A7 as the connector (Figure 11).<sup>28,29</sup> The structural analysis showed that, in 19, three Pt atoms form an approximately equilateral triangle with an average Pt···Pt distance of 13.1 Å. The three edges are slightly bowed outward and the pyridyl rings are canted with respect to the Pt<sub>3</sub> plane. Two isomeric triangles were possible depending on the relative orientations of the unsymmetrical linkers. In the solid state, only the less symmetrical isomer was observed, in which three Pt corners have different coordination environments. The amide groups along the edges were designed to provide orientation through secondary H-bonding perpendicular to the Pt<sub>3</sub> triangle. In fact, in the crystal

structure, pairs of triangular cations stack on top of each other in anti-prismatic fashion, at a distance of 5.1 Å, through pairwise inter-triangle  $\text{NH}\cdots\text{OC}$  H-bonds and  $\text{Pt}\cdots\text{O}=\text{C}$  interactions.



**Fig. 11** Pt based molecular triangles; adapted from ref. 49.

Duan and co-workers<sup>50</sup> have reported a  $\text{Pd}^{2+}$ -based triangle by the reaction of ligand **L8** with  $\text{Pd}(\text{NO}_3)_2$  in 1:1 stoichiometry (Figure 12). The ligand **L8** offers four pyridyl groups as the efficient coordination sites. The hexacationic triangle **20** is comprised of three  $\text{Pd}(\text{II})$  ions and three **L8** ligands. Each  $\text{Pd}(\text{II})$  ion is coordinated by four pyridine groups from two different ligands in a square-planar configuration while each ligand bridges two  $\text{Pd}(\text{II})$  ions alternatively. The  $\text{Pd}\cdots\text{Pd}$  separation within the triangle was found to be 1.27 nm whereas the inner diameter of the cavity was 1.3 nm. The  $\text{O}_{\text{amide}}$  groups were projected outwards whereas the  $\text{N-H}$  bonds were oriented towards the interior of the triangle to form weak H-bonds with the disordered solvent

molecules. Importantly, the resultant porous molecular crystalline solid was utilized for size-selective heterogeneous Knoevenagel condensation reaction.

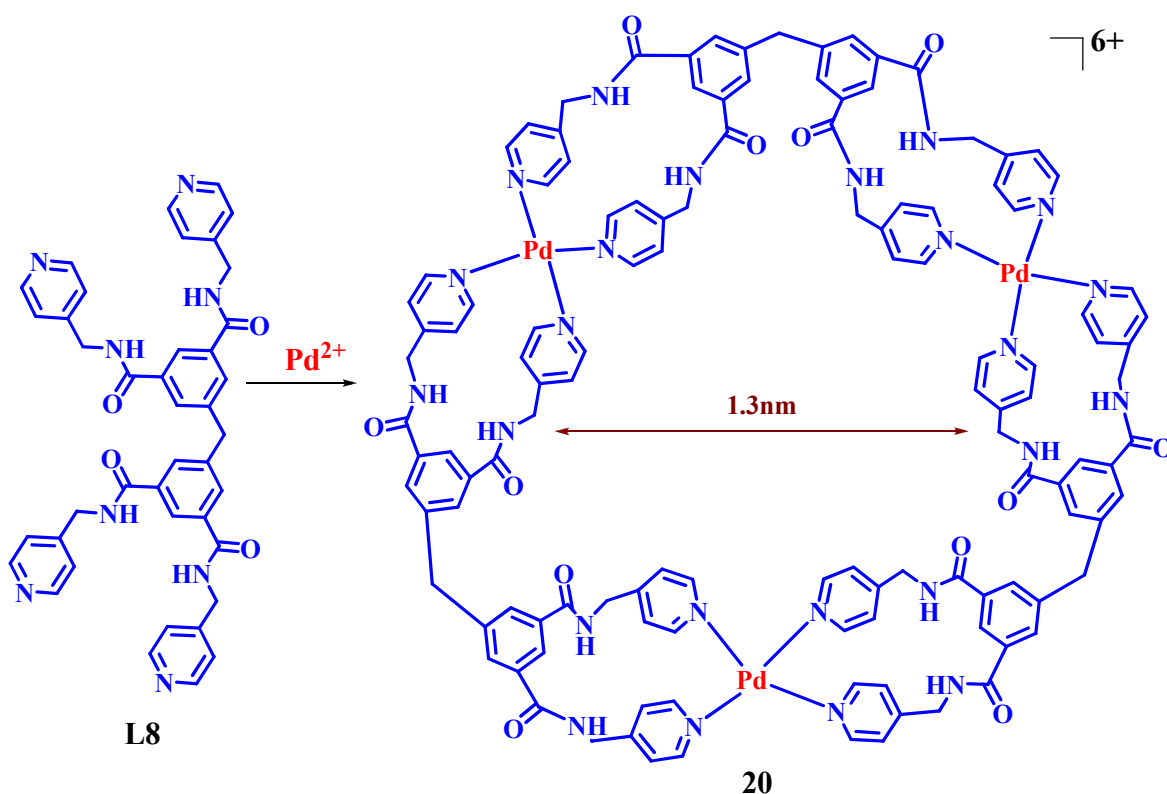
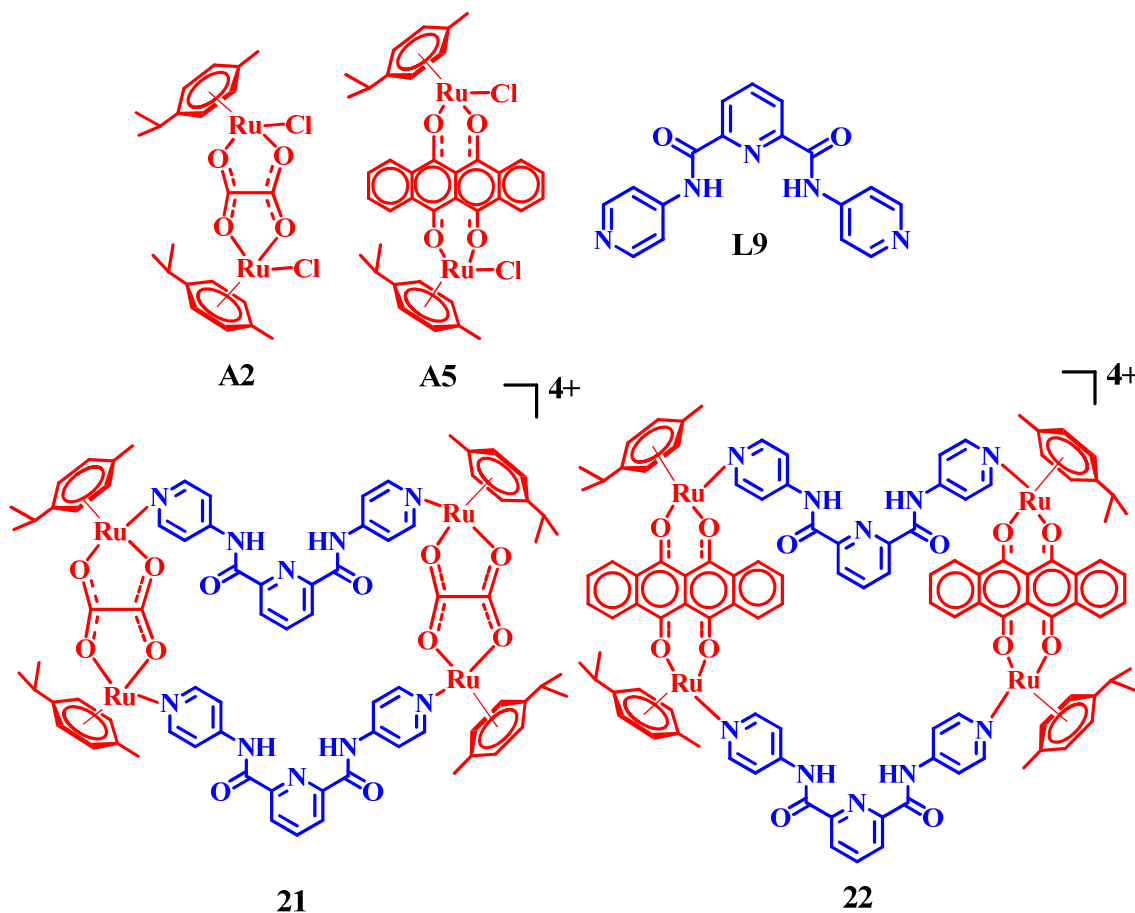


Fig. 12 Pd based molecular triangle; adapted from ref. 50.

#### 6.4 Two-dimensional Metallacycles

With the success of discrete assemblies, several other higher order metallacycles were attempted by using specifically designed pyridine-amide donors with directional rigid ligand capped transition-metal acceptors.<sup>51,52</sup> Chi and co-workers<sup>53</sup> have recently reported tetranuclear tetra-cationic metallabowls **21** and **22** by the self-assembly of bis-pyridyl amide ligand **L9** to that of arene-ruthenium-based acceptors, **A2** and **A5**, respectively (Figure 13). These metallacycles were characterized by NMR and mass spectroscopic methods. The molecular structures for both metallabowls were established by the X-ray diffraction studies. The crystal structure of oxlate-based metallabowl **21** showed that one of the triflate anions was encapsulated at the center of the

cavity through H-bonding. The guest triflate anion was found to tilt to one side of the bowl, which permits only two of its oxygen atoms to interact closely with the amide NHs. Interestingly, this metallabowl was arranged with all NH groups directed inwards and C=O groups directed outward; a fact which excluded C=O groups from the H-bonding.



**Fig. 13** Ru based molecular metallacycles; adapted from ref. 53.

The metallabowl **22** formed using the di-ruthenium clip **A5** was proved to be effective for the anion binding studies. UV-Vis and fluorescence titration studies showed that **22** selectively binds multi-carboxylate anions such as oxalate, tartrate, and citrate in a 1:1 ratio in contrast to mono anions, such as  $F^-$ ,  $Cl^-$ ,  $NO_3^-$ ,  $PF_6^-$ ,  $CH_3COO^-$ , and  $C_6H_5COO^-$ . Metallabowl **22** also acted

as a turn-on fluorescent chemosensor that was suitable for optically and visually detecting biologically important anions, including oxalate, tartrate, and citrate.

Tetra-cationic hetero-bimetallics **23** and **24** were prepared from bis-pyridyl amide ligand **L9** and square-planar Pd(II) and Pt(II) organometallic acceptors **A8** and **A9**, respectively; by Chi and coworkers (Figure 14).<sup>54</sup> Multinuclear NMR and mass spectrometric results, along with single-crystal X-ray analysis confirmed the formation of metallacycles. The <sup>1</sup>H NMR spectra of both metallacycles clearly showed the formation of a symmetrical species with typical resonance shifts for the protons due to metal complexation. The crystal structures of **23** and **24** unambiguously displayed that two pyridyl groups of **L9** are connected with two *cis*-(dppf)M(OTf)<sub>2</sub> (M = Pd or Pt) building blocks to form the [2+2] hetero-bimetallics. The ferrocenyl moieties occupied the outer sites on the partially distorted square-planar M(II) center. Each metal center is coordinated with two phosphorus atoms of ferrocenyl moieties and two nitrogen atoms from two different pyridyl ligands to yield a slightly distorted square-planar geometry around it. The crystal structures of both **23** and **24** showed the encapsulation of an anion (OTf) within the cavity through H-bonding. The photophysical and gel electrophoresis based binding studies revealed that these metallacycles efficiently interacted with DNA. The kinetic experiments revealed that the Pd-based metallacycle has a greater binding affinity for DNA than the Pt one.

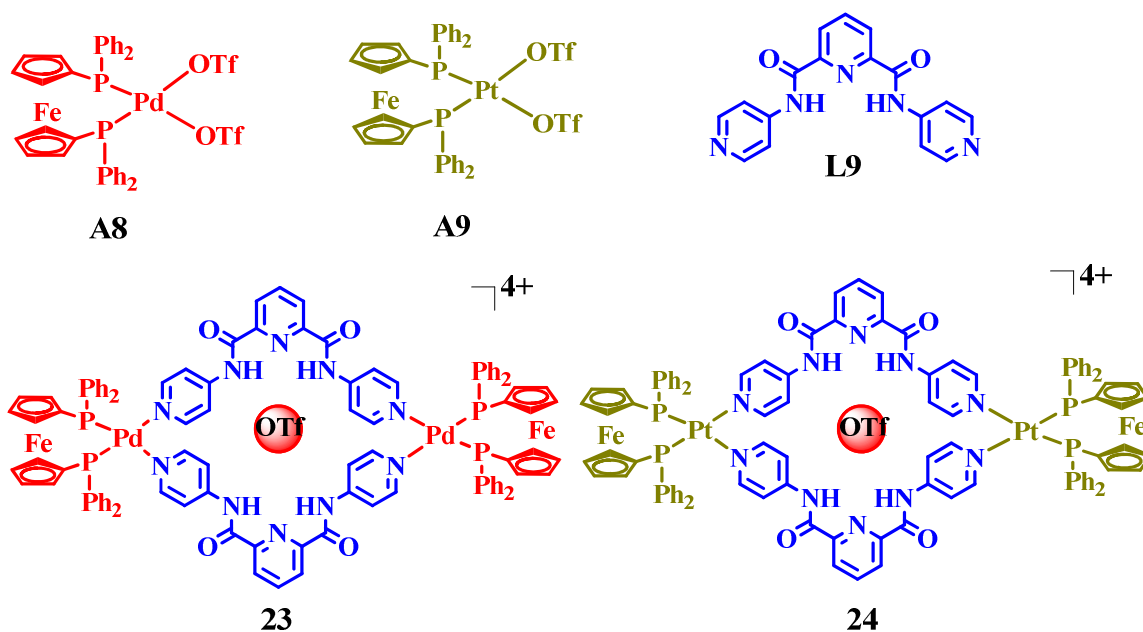


**Fig. 14** Pd and Pt based molecular metallacycles; adapted from ref. 54.

The bis-pyridyl amide ligand **L9** has also been used for the preparation of an unprecedented self-complementary  $\text{Ru}^{2+}$ -based metallacycle with intra-cavity H-bonding interactions. In particular, reaction of  $[\text{RuCl}_2(\text{PPh}_3)_3]$  (**A10**), 1,3-bis(diphenylphosphino)propane, and ligand **L9** yielded the coordination-driven self-assembly of the metallacycle (Figure 15). Reversible dissociation/association behavior of metallacycle **25a** in solution was controlled by the halide ion.<sup>56</sup> The single-crystal X-ray structure of **25a** clearly exhibits an interesting supramolecular association between two severely folded molecules of  $\text{Ru}^{2+}$ -based **25**. The folded metallacycle **25**, self-complementary monomers of **25a**, were oriented orthogonally to each other. This orthogonal assembly was directed by the  $\text{N-H}\cdots\text{Cl-Ru}$  H-bonds. A more definite evidence for the self-complementary assembly of **25a** in solution was confirmed by the  $^1\text{H}$  NMR experiments. To evaluate the relative response of **25a** toward assorted anions,  $^1\text{H}$  NMR titration experiments were carried out by adding other tetraethyl ammonium halide salts. The metallacycle **25a** showed a rather weak response to bromide and a very weak one to iodide

whereas there was no interaction at all with  $\text{NO}_3^-$ ,  $\text{ClO}_4^-$ ,  $\text{BF}_4^-$ , and  $\text{PF}_6^-$ . However, the relative strength to dissociate **25a** into **25** were approximately 2 ( $\text{Br}^-$ ) and 200 ( $\text{I}^-$ ) times weaker than that of  $\text{Cl}^-$  ion. The reversible dissociation/association of self-assembled architectures by chemical stimuli was considered to be a potentially useful property in supramolecular chemistry.

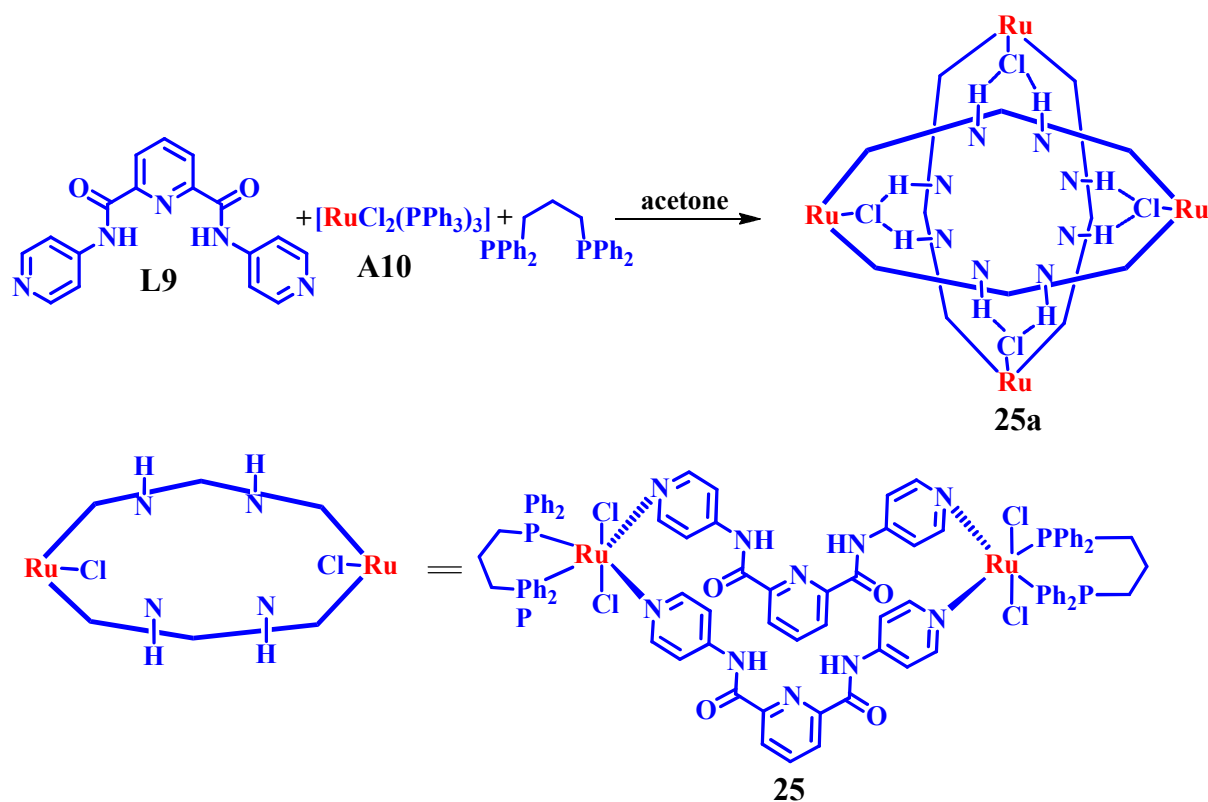


**Fig. 15** Ru based molecular metallacycles; adapted from ref. 56.

Chi and coworkers have used ligand **L10** and molecular clip **A2** for a  $[2 + 2]$  self-assembled metallacycle **26** (Figure 16).<sup>55</sup> The metallacycle **26** was characterized using ESI-MS and NMR spectroscopy as well as by the single crystal X-ray diffraction study. The inclusion of diamide moieties on the wedge-shaped ditopic donor ligands provided the H-bonding sites which suggested potential binding possibilities. Absorption and emission-based titration studies revealed that the metallacycle **26** strongly binds to the enhanced green fluorescent protein

(EGFP), a variant of GFP. This binding was further probed by the gel electrophoresis, circular dichroism and AFM studies which indicated that EGFP undergoes aggregation in the presence of metallacycle **26**. Importantly, such an aggregation was neither noticed for the precursors nor for the related systems that lacked hydrogen bonding functionalities. This study indicated that the metallacycle induces conformational changes to EGFP thus disrupting the tripeptide chromophore. The amide functionalities of **26** appeared essential for the protein interaction and subsequent aggregation which was further supported by the molecular modeling studies. Such modeling studies displayed a favorable interaction, predominantly between metallacycle and Arg-168 residue of EGFP.

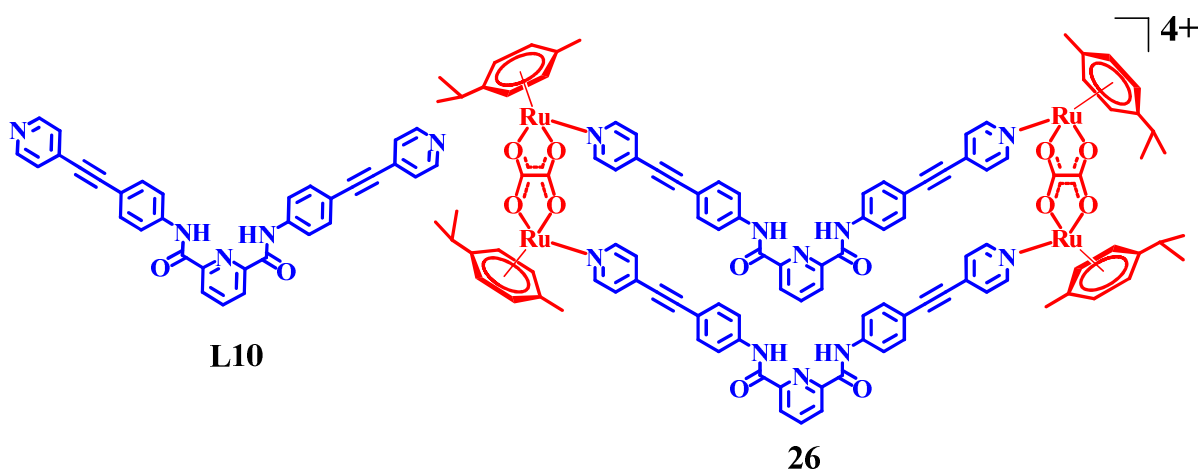


**Fig. 16** Ru based molecular metallacycle; adapted from ref. 55.

Mukherjee and co-workers have synthesized two coordination-driven metallacycles from the carbazole-based dinuclear Pt(II) building block as the acceptors and pyridine-amide ligands as the donors (Figure 17).<sup>57</sup> The treatment of 3,6-bis[trans-Pt(PEt<sub>3</sub>)<sub>2</sub>(NO<sub>3</sub>)(ethynyl)]carbazole **A11** with pyridine-amide donor ligands (**L11** or **L12**) led to the formation of metallacycles **27** and **28**. Multinuclear NMR spectra and ESI-MS studies clearly supported the formation of metallacycles. These metallacycles showed luminescent behavior in solution due to the presence of Pt-ethynyl functionality and conjugated  $\pi$ -electrons. One of these metallacycles containing ligand **L11**

showed its ability to selectively sense pyrophosphate anion. Enhancement of fluorescence intensity was observed upon titration with aqueous pyrophosphate ion in DMF. Notably, the fluorescence intensity almost remains unchanged upon addition of other anions, suggesting a high selectivity towards pyrophosphate ion.

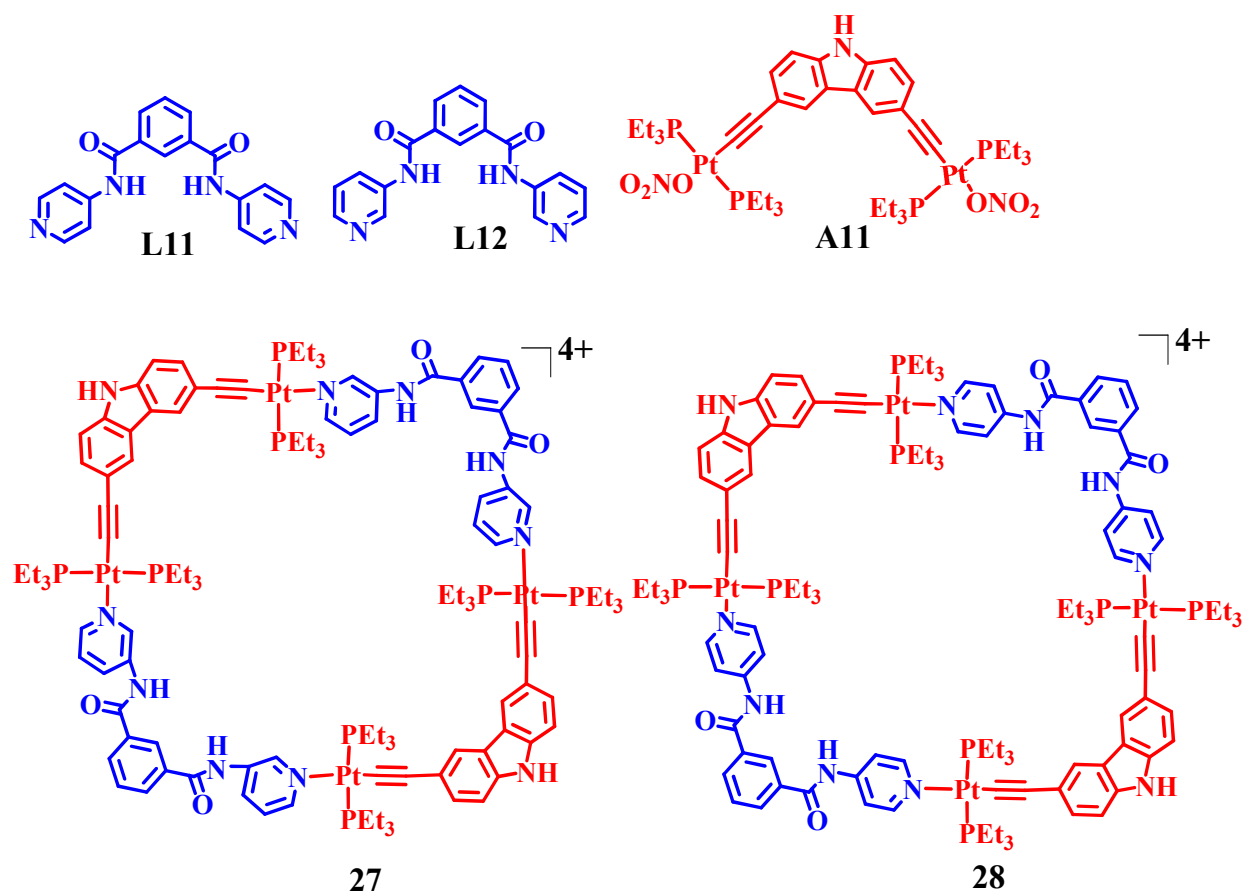
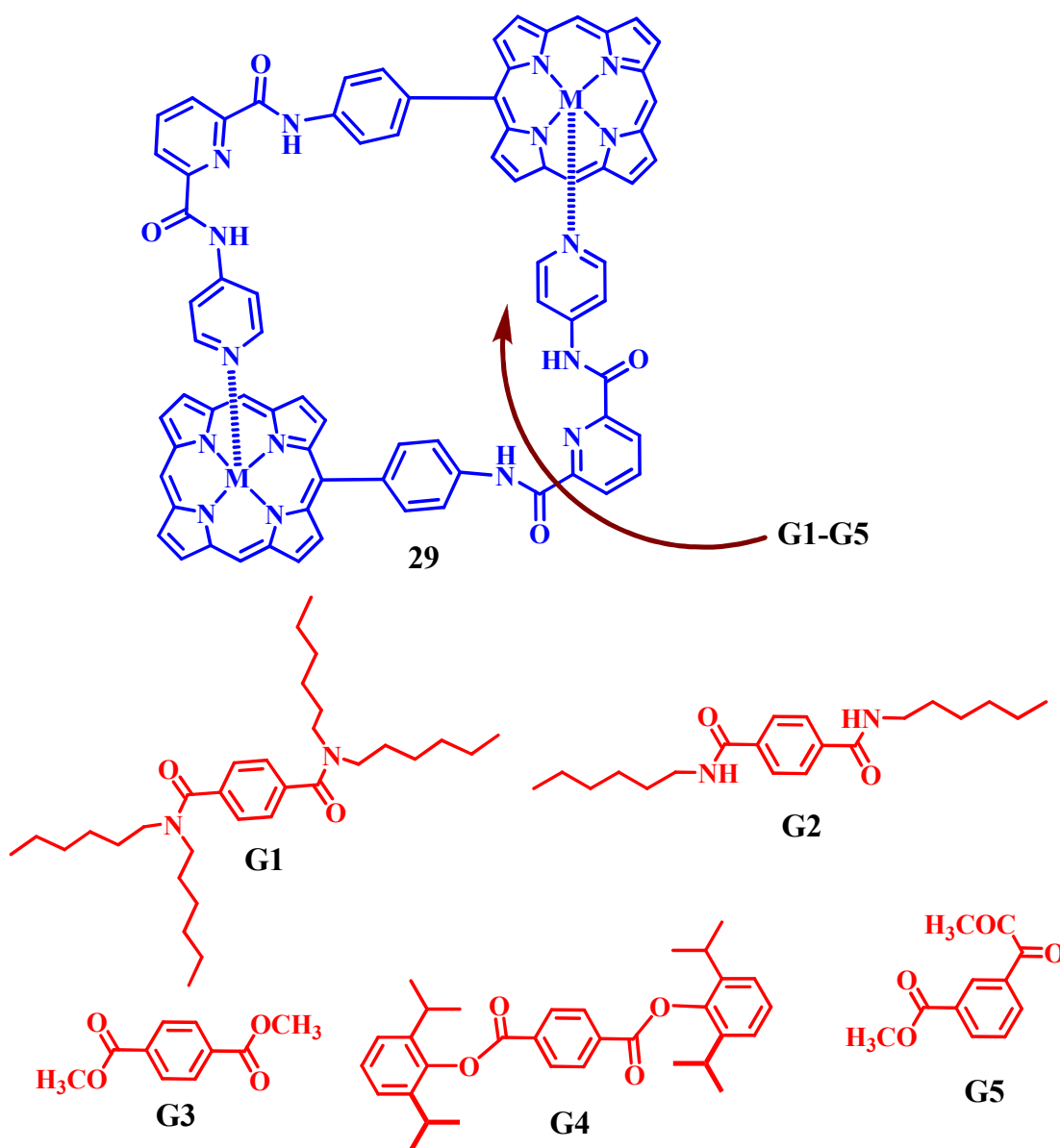


Fig. 17 Pt based molecular metallacycles; adapted from ref. 57.

Hunter and Sarson have reported a pyridine-amide-appended Zn(II)-porphyrin based metallacycle **29** as the host which can encapsulate appropriate terephthalamide derivatives (Figure 18).<sup>58</sup> The metallacycle **29** was characterized by <sup>1</sup>H NMR, FAB-MS, absorption and emission spectroscopy. The functionalized spacious macrocyclic cavity was created through a Lewis acid–base interaction between the Zn(II)-porphyrin and the appended pyridyl rings. The recognition

property of **29** was investigated by  $^1\text{H}$ NMR titration studies with guests **G1-G5** in  $\text{CDCl}_3$ . The metallacycle **29** offers strong intermolecular H-binding sites due to the amide functionality of the pyridine-amide ligand. The amidic guests **G1** and **G2** were bound more strongly than the ester guest **G3**, possibly because of the greater basicity of the  $\text{O}_{\text{amide}}$  atoms. However, guest **G4** inhibits complexation with **29** after increasing steric bulk around the carbonyl group. The isophthalic acid derivatives **G5** was observed to bind to metallacycle very weakly, as the distance between two carbonyl groups is too short for the simultaneous formation of H-bonds to amide groups at both ends of the cavity. Notably, complexation can be observed with the free-base porphyrin, however, the association constants were more than an order of magnitude smaller than those measured for **29**. This work nicely demonstrates the importance of functionalized macrocycles with spacious cavities for selective molecular recognition.



**Fig. 18** Zn(II)-porphyrin based molecular metallacycle; adapted from ref. 58.

Jeong and co-workers<sup>59,60</sup> have reported the self-assembly of a series of discrete, neutral and octahedral Os(VI) based metallacycles **30-32** (Figure 19). These metallacycles possess well-defined cavities enclosed by aryl walls and acted as host molecules. Os(VI)-bridged metallacycles **30a-c**, **31**, and **32** assembled spontaneously when osmium tetroxide, olefins, and L-shaped bis-pyridyl ligands **L13-L15** were mixed in  $\text{CHCl}_3$ . H-bond donors on the inner surface

of the hosts offered binding sites to acceptors of guests with complementary dimensions. The host **30a** binds adipamide ( $K_a = 3.6 \times 10^4 \text{ M}^{-1}$ ) and terephthalamide strongly ( $K_a = 2.0 \times 10^4 \text{ M}^{-1}$ ), while it binds negligibly ( $K_a < 10 \text{ M}^{-1}$ ) benzamide, isophthalamide, or 1,4-naphthalenedicarboxamide. The larger hosts **31** and **32** were able to bind longer guests biphenyl-dicarboxamide and terphenyl-dicarboxamide, respectively, but shorter guests such as adipamide and terephthalamide were not well-bound ( $K_a < 10 \text{ M}^{-1}$ ). These results suggest that two H-bonding sites of **30** must be simultaneously involved in the association with diamide guests. The molecular structure clearly stated that the guest terphenyl-dicarboxamide was complexed inside the cavity of host **30** mainly through H-bonding between host's NHs and guest's carbonyl oxygen atoms. Nevertheless, in the cavity of host **31**, smaller guests such as terephthalamide had the freedom of entering and leaving without sticking ( $K_a = 8 \text{ M}^{-1}$ ) whereas rigid carboxamide was nearly a perfect fit for the space available inside the rectangular box **31** and bound strongly ( $K_a = 4.5 \times 10^4 \text{ M}^{-1}$ ). The chain length selectivity of **31** was shown to be less than that of **30** according to a series of experiments with flexible guests. Moreover, the larger analogue **32** was found to bind larger guest amides, such as dicarboxamide ( $K_a = 7.8 \times 10^2 \text{ M}^{-1}$ ) but lower than those expected for an ideal guest as established by **30** and **31**.

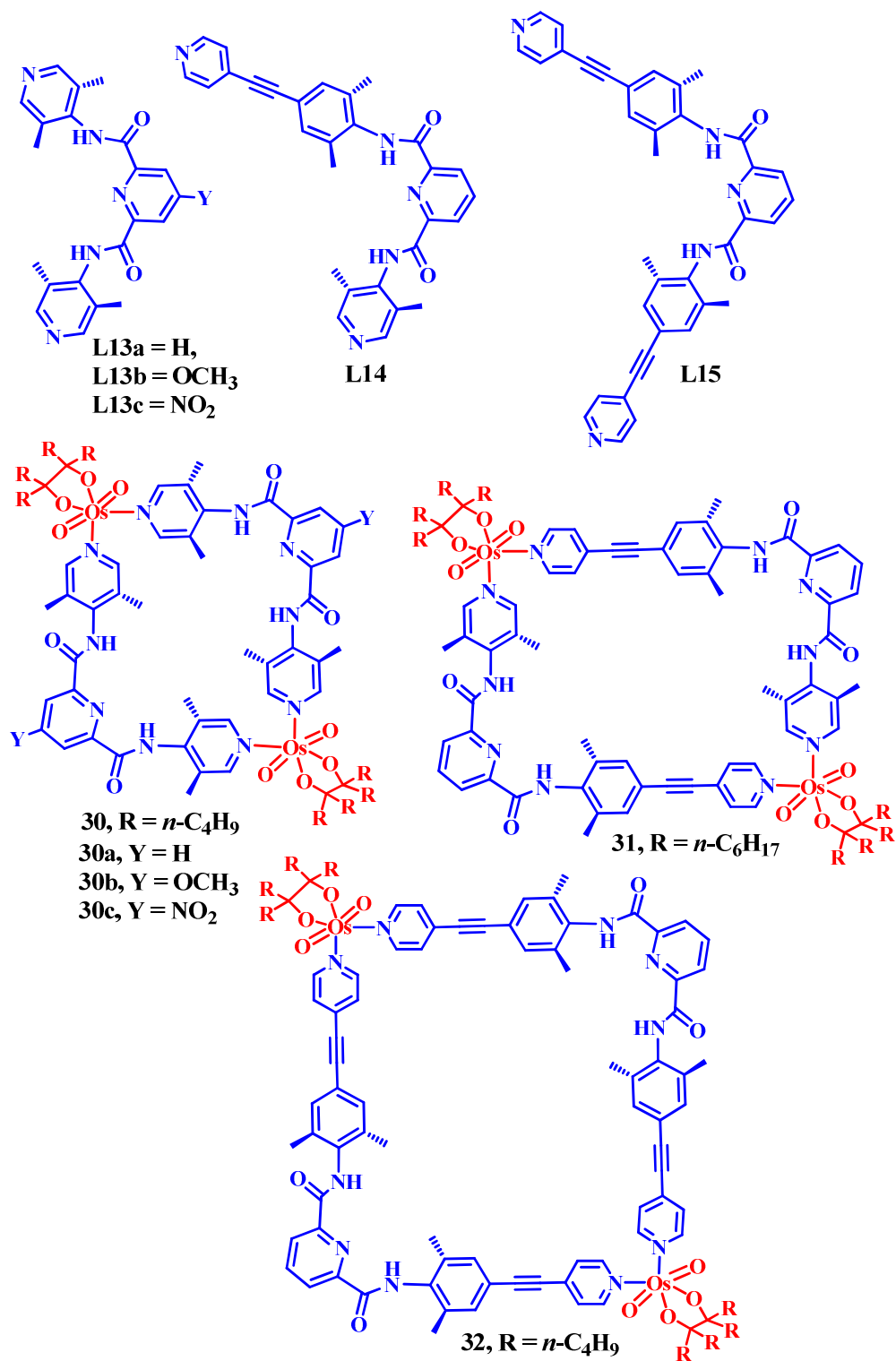


**Fig. 19** Os based molecular metallacycles; adapted from ref. 59 and 60.

Jeong and co-workers<sup>61</sup> have also reported a metallacycle **33** with two topologically discrete binding sub-cavities via pyridine-amide containing ligand **L16** and organometallic moiety, Pd(dppp)OTf<sub>2</sub>, as the acceptor **A12** (Figure 20). This metallacycle was characterized by <sup>1</sup>H NMR spectroscopy, ESI-MS, and elemental analysis. The metallacycle **33** was found to accommodate tetramethyl-terephthalamide guest molecule in each cavity in a cooperative manner with appropriate size, shape and H-bond functionalities. The <sup>1</sup>H NMR titration experiments were performed to evaluate binding affinities between host **33** and guest, tetramethyl-terephthalamide.

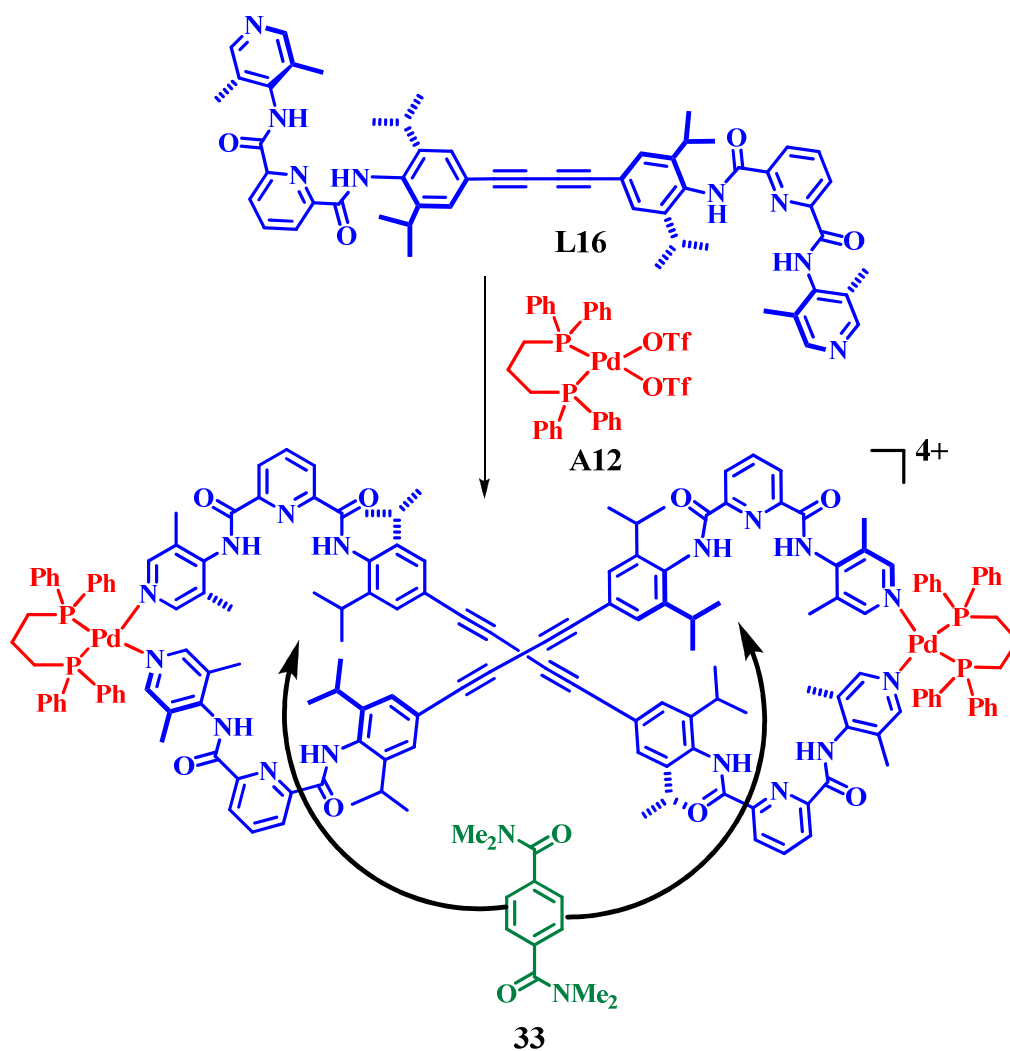
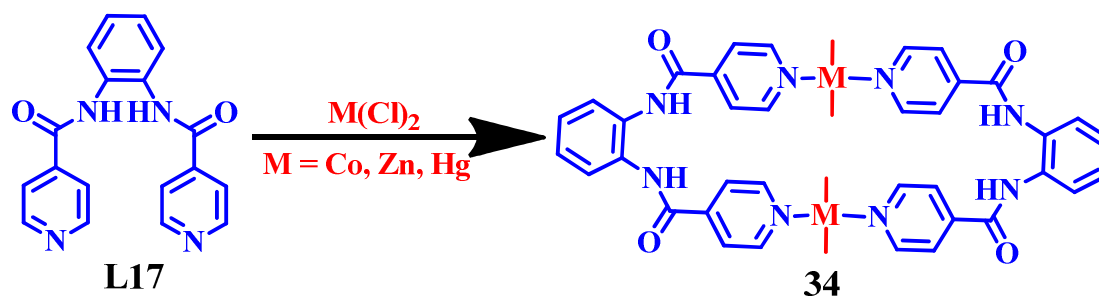


Fig. 20 Pd based molecular metallacycle; adapted from ref. 61.

When the guest tetramethyl-terephthalamide was added, two NH signals of **33** were gradually downfield shifted, indicative of H-bond formation. However, the chemical shift changes were negligible when a monoamide, *N,N*-dimethylbenzamide, was added under the identical conditions. The titration study supported a 1:2 binding isotherm between the host and the guests.

Recently, cobalt, zinc, and mercury containing metallacycles have been synthesized by reacting a dipyridyl-diamide ligand **L17** with metal halide salts (Figure 21).<sup>62</sup> The crystallographic results suggested an interplay between the inclusion of solvent, H-bonding and  $\pi$ - $\pi$  stacking which controls the supramolecular isomerism. There was no ligand-based intramolecular H-bonding between amide groups; instead, two amide groups form an H-bonded dimer and an N-H group forms a further H-bond to a chloride ligand. The remaining two H-bond acceptors, the chloride ligand and carbonyl group, interacted with C-H groups of the pyridyl groups forming an inter-molecular motif in the latter case. These metallacycle showed permanent porosity and single-crystal-to-single-crystal transformations.



**Fig. 21** Co, Zn and Hg based molecular metallacycles; adapted from ref. 62.

In supramolecular self-assembled systems, several factors affect the dynamic equilibrium, such as concentration, temperature, solvent, and ligand flexibility. Both concentration and temperature plays a vital role in the equilibrium of metal-driven self-

assemblies. Although an increase in the concentration shifts the equilibrium towards the formation of high-nuclearity assemblies; an increase in temperature allows the dynamic equilibrium to favor the low-nuclearity species. Vilar and co-workers have reported a dinuclear assembly **35** from a flexible bis-pyridyl ligand **L18** and acceptor **A12** which remains in equilibrium with its higher homologue, the  $M_3L_3$  trinuclear species **36** (Figure 22).<sup>63</sup> The  $^1H$  NMR spectrum in DMSO- $d_6$  exhibited a broad set of signals in addition to another set of signals with lower intensity, which suggested the occurrence of a dynamic process in the solution state. The variable-temperature  $^1H$  NMR spectra exhibited signal sharpening and a shift of few signals. At 350 K, only one set of signals was observed, which correspond to the binuclear assembly **35**, as confirmed later using a dilution experiment. When the concentration of the mixture was gradually decreased, no shift of the signals was detected. However, a change in the integration ratio of two sets of signals was observed. This observation indicated the presence of assemblies with different stoichiometry ( $M_2L_2$  versus  $M_3L_3$ ) rather than different conformations of the complex **35**. The ESI-MS data also supported the presence of two different species,  $M_2L_2$  and  $M_3L_3$ . Although only two different assemblies were observed, it was expected that in presence of a mixture of ligands a larger library of metallacycles could be obtained.

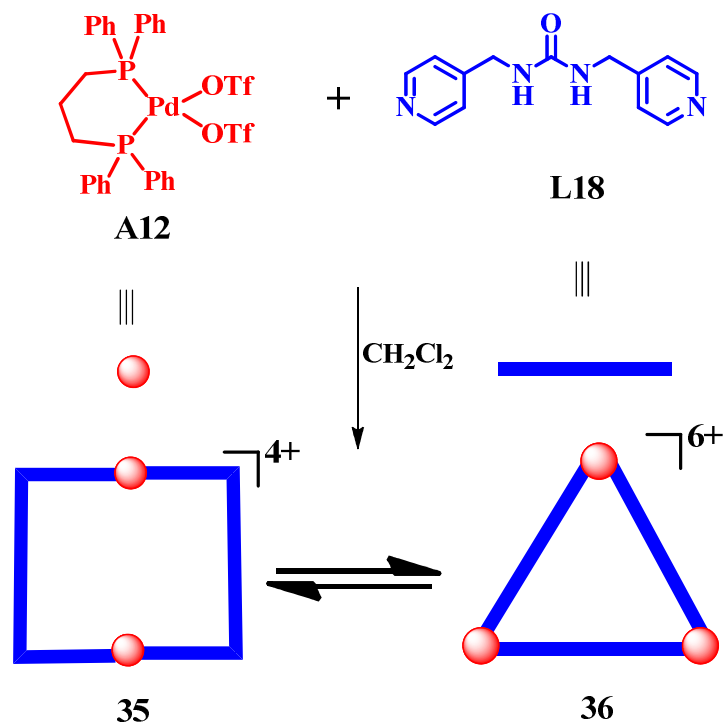


**Fig. 22** Pd based molecular metallacycles ( $M_2L_2$  versus  $M_3L_3$ ); adapted from ref. 63.

## 7. Three-Dimensional Structures

### 7.1 Nanoscopic Cages

The coordination driven self-assembly approach has further been extended to the synthesis of more complex polyhedral three-dimensional (3D) structures. In recent years, a wide range of 3D metallosupramolecular architectures has been utilized for various applications, such as host-guest chemistry, cavity control synthesis, catalysis, magnetic behavior, and sensing.<sup>52,64-66</sup>

Stang and co-workers<sup>66</sup> have synthesized flexible and nanoscopic 3D cages **37a** and **37b** via coordination driven self-assembly using a tripodal amide-based ligand **L19** and  $Pd^{2+}$ -based  $90^\circ$  angular ditopic acceptors **A13a** and **A13b** (Figure 23). Both self-assembled cages were characterized by NMR ( $^{31}P$ ,  $^1H$ ) spectra and mass spectrometry. Notably, when tripodal linkers reacted with  $90^\circ$  ditopic units in a 4:6 ratio; self-assembled double square **37a** was obtained; however, a 2:3 ratio afforded trigonal bipyramid cage **37b**. The double square **37a** and trigonal

bipyramid cage **37b** were easily distinguished by their NMR spectra. A MM2 force field simulation of pseudo trigonal bipyramidal cage showed the diameter of the inner cavity of about 1.9 nm.

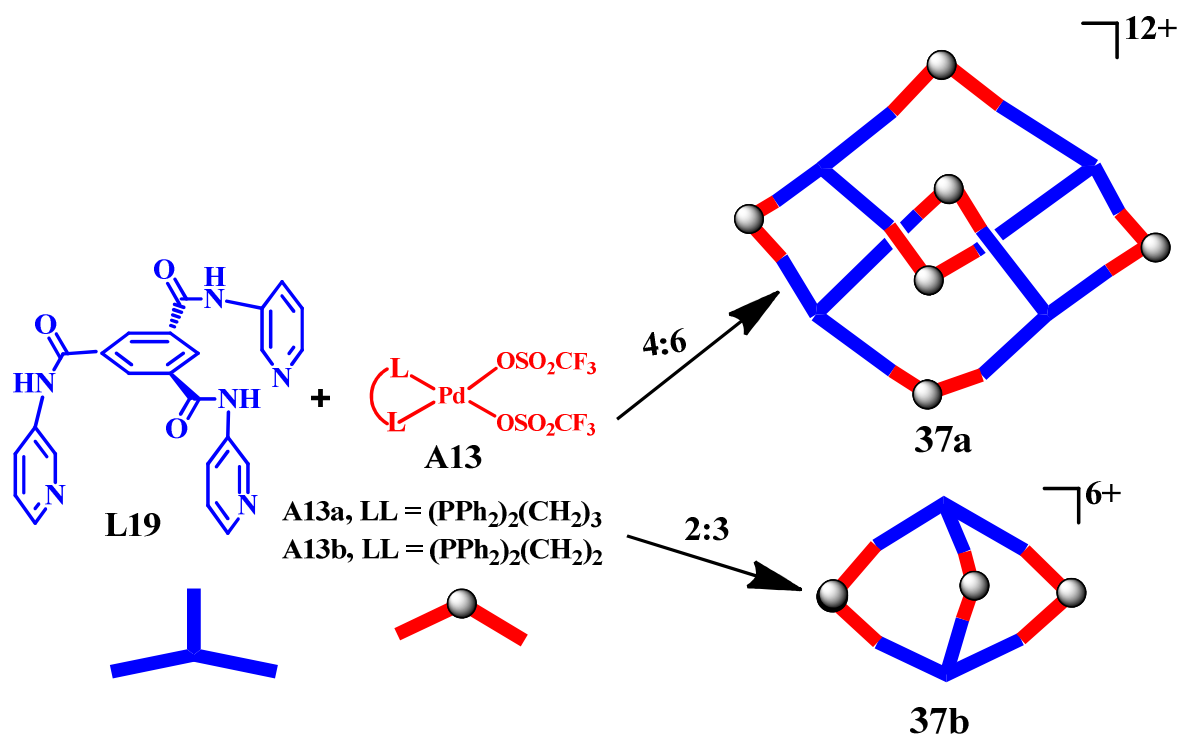
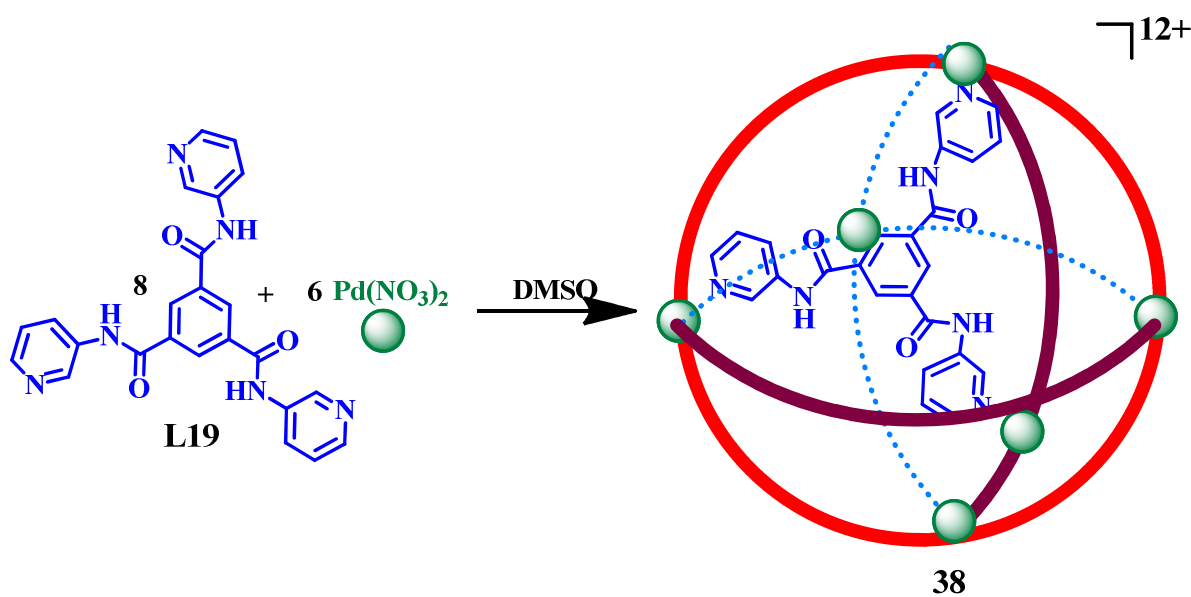


Fig. 23 Pd based molecular cages; adapted from ref. 66.

Lah and co-workers<sup>67</sup> have also reported a nano-sized octahedral cage **38** using a  $C_3$ -symmetric triangular amide-based ligand as the facial component and a  $C_4$ -symmetric  $\text{Pd}^{2+}$  ion as the corner linker. Treatment of four equivalents of **L19** with three equivalents of  $\text{Pd}(\text{NO}_3)_2$  led to the quantitative self-assembly of a single product as determined by  $^1\text{H}$  NMR spectroscopy (Figure 24). Crystallographic studies revealed that 3-pyridyl atoms of the triangular ligand provided the needed curvature for the formation of a molecular sphere. The curvature needed for the truncation at the octahedral vertices was accomplished using **L19** with a tilted pyridyl group and a nitrogen donor atom in a  $\sim 120^\circ$  kink (Figure 24). These face-driven corner-linked nano-

cages have twelve ports at the edges of the truncated octahedron. Notably, depending on the size of the facial ligands, not only the cavity size but also the port size of the cage could be controlled. Using a similar approach, a  $\text{Pd}^{2+}$ -based molecular sphere incorporating ester functionalities in place of amide groups in **L19**, was assembled using a  $C_3$ -symmetric tripodal linker,  $N,N',N''$ -tris(4-pyridylmethyl)trimesic ester, with  $\text{Pd}(\text{NO}_3)_2$  in 4:3 ratio. NMR, ESI-MS, TEM, and MM2 force-field calculations supported the formation of the nanoball with eight trigonal faces occupied by the  $C_3$ -symmetric donor linkers. These results suggest the potential possibilities of developing nano-sized hosts that can accommodate suitable small molecular guests or even chiral catalysts.<sup>68</sup>



**Fig. 24** Pd based nano-sized molecular cage; adapted from ref. 67.

Water clusters can play an important role in the stabilization of supramolecular systems both in solution and in the solid state. In this regard Atwood and co-workers<sup>69</sup> have demonstrated a self-assembled 3D supramolecular cage **39** that was stabilized by an intricate array of non-covalent interactions involving contributions from water clusters, most notably a water decamer

$(\text{H}_2\text{O})_{10}$  with an ice-like molecular arrangement (Figure 25). The crystal structure of **39** reveals a dinuclear pseudo-macrotricyclic complex in which two octahedral  $\text{M}^{2+}$  ions ( $\text{M} = \text{Co}$  or  $\text{Cu}$ ) are linked by four bridging pyridine-amide based ligand **L20** to form a molecular cage. All four equatorial positions on each metal centre were occupied by the pyridyl groups while the axial positions by the coordinated water molecules. The structure contains two crystallographically unique water decamers located within the cage. Eight H-bonds were formed between the water decamer and the amide groups and nitrate anions of adjacent linear arrays and contributed to the stabilization of overall structure. These findings nicely illustrate that the degree of structuring could be imposed on water molecules by its surroundings and vice versa and such an effect could be profound and may control the overall architecture.

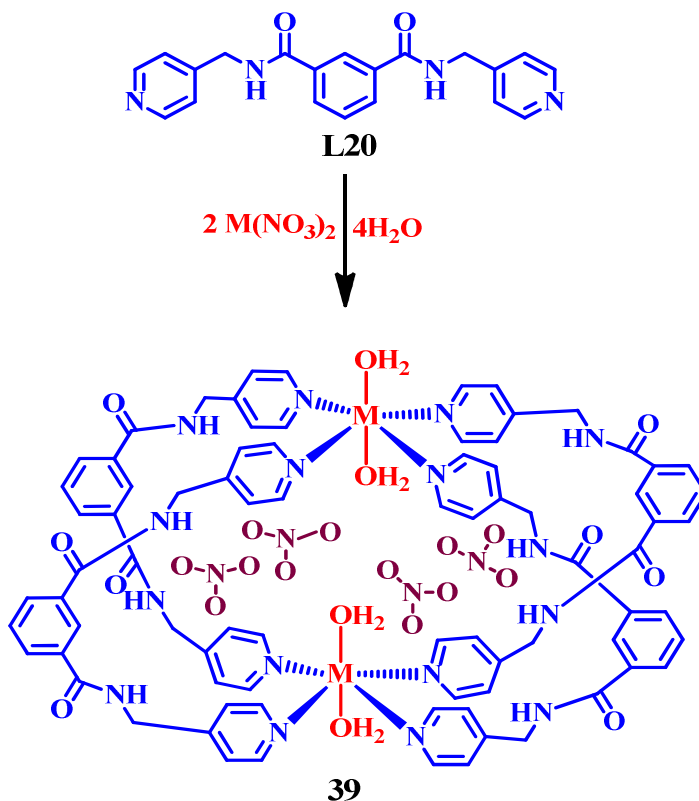


**Fig. 25** Cu and Co based molecular cages; adapted from ref. 69.

## 7.2 Molecular Prisms

The use of tritopic planar metal-based acceptors in combination with 0° organic clips has been shown for the formation of trigonal prisms.<sup>70-73</sup> Mukherjee and co-workers have reported a few trigonal prisms using pyridine-amide ligands as donor and organometallic acceptors via self-assembly (Figure 26).<sup>73</sup> A nanoscale structure **40** with trigonal prismatic shape was prepared by coordination-driven self-assembly of a predesigned organometallic Pt<sub>3</sub> acceptor **A14** with a pyridine-amide “clips” donor ligand **L12**. Multinuclear NMR and mass spectra confirmed the formation of trigonal prism. Incorporation of Pt-ethynyl functionality makes the prism fluorescent in nature. In addition, the conjugated ethynyl functionalities make the molecular prism  $\pi$ -electron-rich for the detection of electron-deficient nitro-aromatics. The fluorescent intensity of molecular prism **40** was quenched upon addition of electron-deficient tri-nitro toluene (TNT), a well-known explosive.

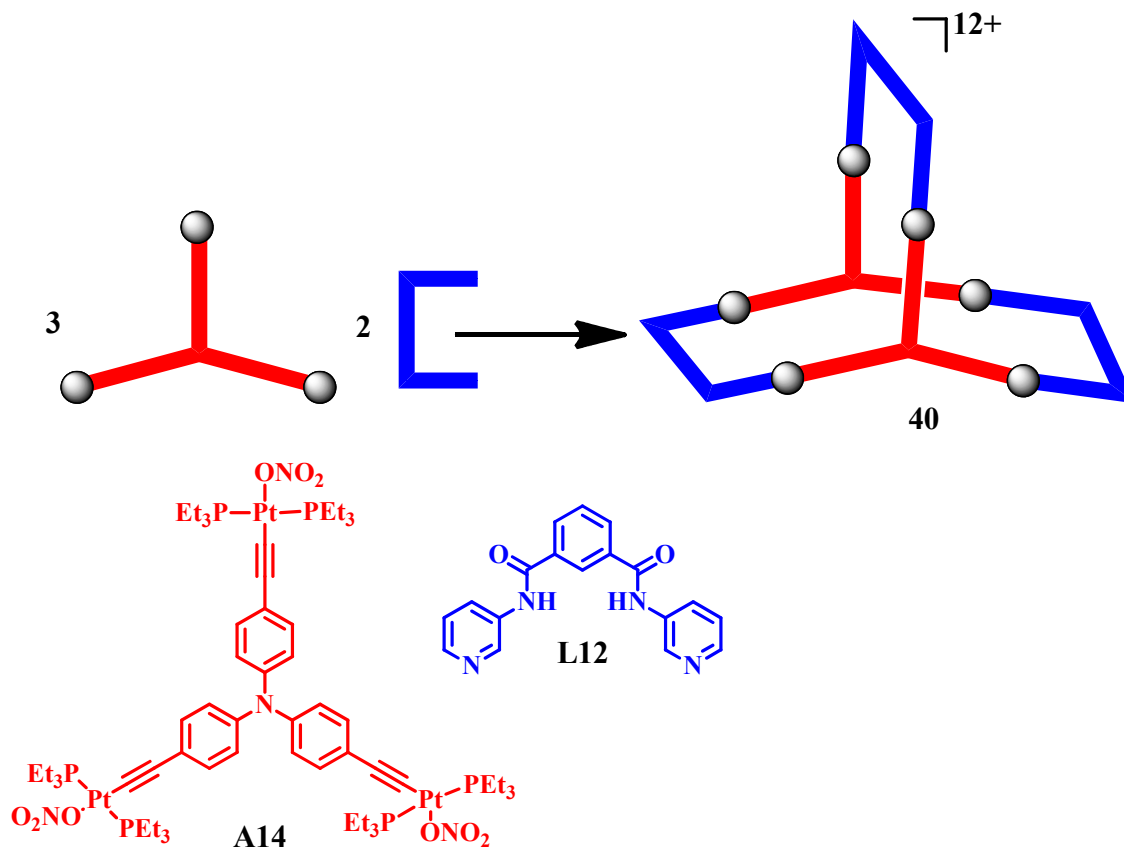


Fig. 26 Pt based molecular prism; adapted from ref. 73.

## 8. Concluding remarks and future prospects.

This short review has outlined the recent supramolecular coordination chemistry of pyridine-amide ligands. A variety of architectural shapes including rectangles, squares, triangles, cages, and prisms are shown to be constructed solely by the self-assembly employing designed pyridine-amide based ligands. The examples collected in the present review amply highlight the importance of pyridine-amide based ligands for their unique abilities to not only offer structural flexibility and their capability to adjust to the geometrical requirement of the metal ion essential for the construction of a supramolecular structure but also their propensity to offer assorted

functional groups. A suitable combination of such parameters generates a range of interesting ligands with assorted architectural possibilities.

In addition to aesthetic importance; such architectures are shown to offer a number of applications. Such applications vary from biology, such as DNA binding and anticancer activity; to chemistry, for instance sensing and host-guest interactions. Particularly, biomedical applications of such designed architectures for their potentials as the antitumor agents; sensors for protein, enzymes, nucleic acid, etc. open new vistas that are likely to further flourish. Although decent advances have been made in the creation of pyridine-amide based supramolecular architectures; this field is still in its infancy especially towards architecture-dependent applications. The novel yet predictable architectures and their tailor-made applications are anticipated to remain a productive discipline for greater exploration and creativity.

**Acknowledgments.** RG thanks SERB, Govt. of India, New Delhi for the continuous financial support. AM is grateful to Department of Science and Technology (DST), New Delhi for the Young Scientist Project (Project No. SB/FT/CS-103/2012) and Prof. Sandeep Verma for providing lab facilities at IIT Kanpur.

### References.

- (1) J.-M. Lehn, *Angew Chem Int Ed.*, 1988, **27**, 89.
- (2) J.-M. Lehn, *Science* 2002, **295**, 2400.
- (3) D. N. Reinhoudt and M. Crego-Calama, *Science* 2002, **295**, 2403.
- (4) O. Ikkala and G. T. Brinke, *Science* 2002, **295**, 2407.
- (5) M. D. Hollingsworth, *Science* 2002, **295**, 2410.

- (6) T. Kato, *Science* 2002, **295**, 2414.
- (7) G. M. Whitesides and B. Grzybowski, *Science* 2002, **295**, 2418.
- (8) J. A. A. W. Elemans, A. E. Rowan and R. J. M. Nolte, *J. Mater. Chem.* 2003, **13**, 2661.
- (9) J. W. Steed and J. L. Atwood, *Supramolecular Chemistry*; John Wiley & Sons: West Sussex, U.K., 2000.
- (10) (a) T. R. Cook, Y.-R. Zheng and P. J. Stang, *Chem. Rev.*, 2013, **113**, 734. (b) G. Kumar and R. Gupta, *Chem. Soc. Rev.*, 2013, **42**, 9403. (c) G. Ferey, *Chem. Soc. Rev.*, 2008, **37**, 191.
- (11) J. E. Beves and D. A. Leigh, *Nat. Chem.*, 2010, **2**, 708.
- (12) L. Fang, M. A. Olson, D. Benítez, E. Tkatchouk, W. A. Goddard III and J. F. Stoddart, *Chem. Soc. Rev.*, 2010, **39**, 17.
- (13) S. Durot, F. Reviriego and J.-P. Sauvage, *Dalton Trans.*, 2010, **39**, 10557
- (14) S. De, K. Mahata and M. Schmittel, *Chem. Soc. Rev.*, 2010, **39**, 1555.
- (15) P. J. Stang and D. H. Cao, *J. Am. Chem. Soc.*, 1994, **116**, 4981.
- (16) P. J. Stang, B. Olenyuk, J. Fan and A. M. Arif, *Organometallics* 1996, **15**, 904.
- (17) J. A. Whiteford, C. V. Lu and P. J. Stang, *J. Am. Chem. Soc.*, 1997, **119**, 2524.
- (18) M. D. Pluth, R. G. Bergman and K. N. Raymond, *Acc. Chem. Res.*, 2009, **42**, 1650.
- (19) M. D. Pluth, and K. N. Raymond *Chem. Soc. Rev.*, 2007, **36**, 161.
- (20) D. L. Caulder and K. N. Raymond, *J. Chem. Soc. Dalton Trans.*, 1999, 1185.
- (21) T. Murase, S. Horiuchi and M. Fujita, *J. Am. Chem. Soc.*, 2010, **132**, 2866.
- (22) M. Yoshizawa, J. K. Klosterman and M. Fujita, *Angew. Chem., Int. Ed.*, 2009, **48**, 3418.
- (23) M. Fujita, M. Tominaga, A. Hori and B. Therrien, *Acc. Chem. Res.*, 2005, **38**, 369.
- (24) (a) B. Therrien, G. Süss-Fink, P. Govindaswamy, A. K. Renfrew and P. J. Dyson, *Angew. Chem. Int. Ed.*, 2008, **47**, 3773. (b) P. Govindaswamy, D. Linder, J. Lacour, S. Süss-Fink, B.

Therrien, *Chem. Commun.* 2006, 4691. (c) A. Pitto-Barry, N. P. E. Barry, O. Zava, R. Deschenaux, P. J. Dyson and B. Therrien, *Chem.–Eur. J.*, 2011, **17**, 1966.

(25) Bruno Therrien, *Eur. J. Inorg. Chem.*, 2009, 2445.

(26) (a) J. Mattsson, O. Zava, A. K. Renfrew, Y. Sei, K. Yamaguchi, P. J. Dyson, B. Therrien, *Dalton Trans.*, 2010, **39**, 8248. (b) N. P. E. Barry, N. H. Abd Karim, R. Vilarand and B. Therrien, *Dalton Trans.*, 2009, 10717.

(27) Z. Qin, M. C. Jennings and R. J. Puddephatt, *Chem. Commun.*, 2002, 354.

(28) Z. Qin, M. C. Jennings and R. J. Puddephatt, *Chem. Commun.*, 2001, 2676.

(29) Z. Qin, M. C. Jennings and R. J. Puddephatt, *Inorg. Chem.*, 2003, **42**, 1956.

(30) (a) A. Mishra, N. K. Kaushik, A. K. Verma, and R. Gupta, *Eur. J. Med. Chem.* 2008, **43**, 2189. (b) A. Mishra, A. Ali, S. Upreti, and R. Gupta, *Inorg. Chem.* 2008, **47**, 154. (c) A. Mishra, A. Ali, S. Upreti, M. S. Whittingham and R. Gupta, *Inorg. Chem.*, 2009, **48**, 5234. (d) A. P. Singh, A. Ali, and R. Gupta, *Dalton Trans.* 2010, **39**, 8135. (e) A. P. Singh, G. Kumar, and R. Gupta, *Dalton Trans.* 2011, **40**, 12454. (f) G. Kumar and R. Gupta, *Inorg. Chem.* 2012, **51**, 5497. (g) G. Kumar and R. Gupta, *Inorg. Chem.* 2013, **52**, 10773. (h) A. Ali, G. Hundal, and R. Gupta, *Cryst. Growth Des.* 2012, **12**, 1308. (i) G. Kumar, H. Aggarwal, and R. Gupta, *Cryst. Growth Des.* 2013, **13**, 74.

(31) S. Ghosh and P. S. Mukherjee, *Dalton Trans.*, 2007, 2542.

(32) S. Shanmugaraju, A. K. Bar, S. A. Joshi, Y. P. Patil and P. S. Mukherjee, *Organometallics*, 2011, **30**, 1951.

(33) A. Mishra, H. Jung, J. W. Park, H. K. Kim, H. Kim, P. J. Stang and K.-W. Chi, *Organometallics* 2012, **31**, 3519.

- (34) A. Mishra, S. Lee, H. Kim, T. R. Cook, P. J. Stang and K.-W. Chi *Chem. Asian J.*, 2012, **7**, 2592.
- (35) V. Vajpayee, Y. H. Song, M. H. Lee, H. Kim, M. Wang, P. J. Stang and K.-W. Chi, *Chem. – Eur. J.*, 2011, **17**, 7837.
- (36) V. Vajpayee, Y. H. Song, Y. J. Yang, S. C. Kang, H. Kim, I. S. Kim, M. Wang, P. J. Stang, and K.-W. Chi, *Organometallics*, 2011, **30**, 3242.
- (37) A. Mishra, H. Jung, M. H. Lee, M. S. Lah and K.-W. Chi, *Inorg. Chem.*, 2013, **52**, 8573.
- (38) A. Mishra, Y. J. Jeong, J.-H. Jo, S. C. Kang, H. Kim and K.-W. Chi, *Organometallics*, DOI: 10.1021/om401042m.
- (39) A. Mishra, Y. J. Jeong, J.-H. Jo, S. C. Kang, M. S. Lah and K.-W. Chi, *ChemBioChem*, 2014, DOI: 10.1002/cbic.201300688.
- (40) R. Chakrabarty, P. S. Mukherjee and P. J. Stang, *Chem. Rev.*, 2011, **111**, 6810.
- (41) P. Thanasekaran, R.-T. Liao, Y.-H. Liu, T. Rajendran, S. Rajagopal and K.-L. Liu, *Coord. Chem. Rev.*, 2005, **249**, 1085.
- (42) C. J. Kuehl, S. D. Huang and P. J. Stang, *J. Am. Chem. Soc.*, 2001, **123**, 9634.
- (43) M. J. E. Resendiz, J. C. Noveron, H. Disteldorf, S. Fischer and P. J. Stang, *Org. Lett.*, 2004, **6**, 651.
- (44) F. Würthner, C. C. You and C. R. Saha-Möller, *Chem. Soc. Rev.*, 2004, **33**, 133.
- (45) M. Fujita, J. Yazaki and, K. Ogura, *J. Am. Chem. Soc.*, 1990, **112**, 5645.
- (46) K. Uemura, S. Kitagawa, K. Fukui and K. Saito, *J. Am. Chem. Soc.*, 2004, **126**, 3817.
- (47) B. -C. Tzeng, B -S. Chen, S -Y. Lee, W -H. Liu, G -H. Lee and S -M. Peng, *New J. Chem.*, 2007, **31**, 202.
- (48) M. Capo', J. Benet-Buchholz and P. Ballester, *Inorg. Chem.*, 2008, **47**, 10190.

- (49) B. Lippert and P. J. Sanz Miguel, *Chem. Soc. Rev.*, 2011, **40**, 4475.
- (50) Y. Liu, R. Zhang, C. He, D. Dang and C. Duan, *Chem. Commun.*, 2010, **46**, 746.
- (51) S. Leininger, B. Olenyuk and P. J. Stang, *Chem. Rev.*, 2000, **100**, 853.
- (52) A. Mishra, S. C. Kang and K.-W. Chi, *Eur. J. Inorg. Chem.*, 2013, 5222.
- (53) A. Mishra, V. Vajpayee, H. Kim, M. H. Lee, H. Jung, M. Wang, P. J. Stang and K.-W. Chi, *Dalton Trans.*, 2012, **41**, 1195.
- (54) A. Mishra, S. Ravikumar, S. H. Hong, H. Kim, V. Vajpayee, H. W. Lee, B. C. Ahn, M. Wang, P. J. Stang and K.-W. Chi, *Organometallics* 2011, **30**, 6343.
- (55) A. Mishra, S. Ravikumar, Y. Song, N. S. Prabhu, S. H. Hong, H. Kim, S. Cheon, J. Noh and K.-W. Chi, *Dalton Trans.*, 2014, DOI: 10.1039/C3DT53186D.
- (56) Y. J. Park, J.-S. Kim, K.-T. Youm, N.-K. Lee, J. Ko, H.-S. Park and M.-J. Jun, *Angew. Chem., Int. Ed.*, 2006, **45**, 4290.
- (57) S. Shanmugaraju, A. K. Bar, K.-W. Chi and P. S. Mukherjee, *Organometallics* 2010, **29**, 2971.
- (58) C. A. Hunter and L. D. Sarson, *Angew. Chem., Int. Ed. Engl.*, 1994, **33**, 2313.
- (59) K.-S. Jeong, Y. L. Cho, S.-Y. Chang, T.-Y. Park and J. U. Song, *J. Org. Chem.*, 1999, **64**, 9459.
- (60) K.-S. Jeong, Y. L. Cho, J. U. Song, H.-Y. Chang and M.-G. Choi, *J. Am. Chem. Soc.*, 1998, **120**, 10982.
- (61) S.-Y. Chang, M.-C. Um, H. Uh, H.-Y. Jang and K.-S. Jeong, *Chem. Commun.*, 2003, 2026.
- (62) C. D. Jones, J. C. Tan and G. O. Lloyd, *Chem. Commun.*, 2012, **48**, 2110.
- (63) P. Diaz, J. A. Tovilla, P. Ballester, J. B.-Buchholz and R. Vilar, *Dalton Trans.*, 2007, 3516.

- (64) M. M. J. Smulders, I. A. Riddell, C. Browne and J. R. Nitschke, *Chem. Soc. Rev.*, 2013, **42**, 1728.
- (65) B. J. Holliday and C. A. Mirkin, *Angew. Chem.* 2001, **113**, 2076. *Angew. Chem., Int. Ed.* 2001, **40**, 2022.
- (66) P. S. Mukherjee, N. Das and P. J. Stang, *J. Org. Chem.*, 2004, **69**, 3526.
- (67) D. Moon, S. Kang, J. Park, K. Lee, R. P. John, H. Won, G. H. Seong, Y. S. Kim, G. H. Kim, H. Rhee and M. S. Lah, *J. Am. Chem. Soc.*, 2006, **128**, 3530.
- (68) S. Ghosh and P. S. Mukherjee, *J. Org. Chem.* 2006, **71**, 8412.
- (69) L. J. Barbour, G. W. Orr, and J. L. Atwood, *Nature*, 1998, **393**, 671.
- (70) K. Kumazawa, K. Biradha, T. Kusukawa, T. Okano and M. Fujita, *Angew. Chem., Int. Ed.*, 2003, **42**, 3909.
- (71) K. Ono, M. Yoshizawa, T. Kato, K. Watanabe and M. Fujita, *Angew. Chem., Int. Ed.*, 2007, **46**, 1803.
- (72) S. Ghosh and P. S. Mukherjee, *Organometallics* 2008, **27**, 316.
- (73) S. Ghosh, B. Gole, A. K. Bar and P. S. Mukherjee, *Organometallics* 2009, **28**, 4288.

**Abbreviations for the Ligands:**

*N*-(4-pyridinyl)isonicotinamide (**L1**)

*N*-(4-(pyridin-4-ylethynyl)phenyl)isonicotinamide (**L2**)

*N,N'*-di-(pyridin-4-yl)oxalamide (**L3**)

*N,N'*-di(pyridin-3-yl)oxalamide (**L4**)

*N,N'*-bis(4-(pyridin-4-ylethynyl)phenyl)terephthalamide (**L5**)

*N*-(2-(pyridin-4-yl)ethyl)isonicotinamide (**L6**)

*N,N'*-bis(3,5-dimethyl-4-pyridinyl)-4-ethoxy-2,6-pyridinedicarboxamide (**L7**)

3,3',5,5'-tetra[*N*-(4-pyridyl)methylcarboxylamide]diphenylmethane (**L8**)

*N,N'*-di(pyridin-4-yl)pyridine-2,6-dicarboxamide (**L9**)

*N,N'*-bis(4-(pyridin-4-ylethynyl)phenyl)pyridine-2,6-dicarboxamide (**L10**)

*N,N'*-di(pyridin-4-yl)isophthalamide (**L11**)

*N,N'*-di(pyridin-3-yl)isophthalamide (**L12**)

*N,N'*-bis(3,5-dimethylpyridin-4-yl)-pyridine-2,6-dicarboxamide (**L13**)

*N*-(3,5-dimethylpyridin-4-yl)-*N'*-(4-(pyridin-4-yl-ethynyl)-2,6-dimethylphenyl)pyridine-2,6-dicarboxamide (**L14**)

*N,N'*-bis(4-(pyridin-4-yl-ethynyl)-2,6-dimethylphenyl)pyridine-2,6-dicarboxamide (**L15**)

*N,N'*-(4,4'-(buta-1,3-diyne-1,4-diyl)bis(2,6-diisopropyl-4,1-phenylene))bis(*N*6-(3,5-dimethylpyridin-4-yl)pyridine-2,6-dicarboxamide) (**L16**)

*N,N'*-(1,2-phenylene)diisonicotinamide (**L17**)

1,3-bis(pyridin-4-ylmethyl)urea (**L18**)

*N,N',N''*-tris(pyridin-3-yl)pyridine-1,3,5-tricarboxamide (**L20**)

*N<sup>l</sup>,N<sup>3</sup>*,-bis(pyridine-4-ylmethyl)isophthalamide (**L20**)

**Abbreviations for the Metal Complexes:**

1,8-bis[*trans*-Pt(PEt<sub>3</sub>)<sub>2</sub>(NO<sub>3</sub>)]anthracene (**A1**)

[(Ru<sub>2</sub>(μ-η<sup>4</sup>-C<sub>2</sub>O<sub>4</sub>)(η<sup>6</sup>-*p*-cymene)<sub>2</sub>](Cl)<sub>2</sub> (**A2**)

[Ru<sub>2</sub>(2,5-dihydroxy-1,4-benzoquinonato)(η<sup>6</sup>-*p*-cymene)<sub>2</sub>](Cl)<sub>2</sub> (**A3**)

[Ru<sub>2</sub>(5,8-dioxydo-1,4-naphthaquinonato)(η<sup>6</sup>-*p*-cymene)<sub>2</sub>](Cl)<sub>2</sub> (**A4**)

[Ru<sub>2</sub>(6,11-dihydroxy-5,12-naphthacene dionato)(η<sup>6</sup>-*p*-cymene)<sub>2</sub>](Cl)<sub>2</sub> (**A5**)

*cis*-[Pt(dppp)(O<sub>3</sub>SCF<sub>3</sub>)<sub>2</sub>], dppp = 1,3-Bis(diphenylphosphino)propane (**A6**)

*cis*-[Pt(bu<sub>2</sub>bipy)(O<sub>3</sub>SCF<sub>3</sub>)<sub>2</sub>], bu<sub>2</sub>bipy = 4,4'-*di-tert*-butyl-2,2'-bipyridine (**A7**)

*cis*-[(dppf)Pd(OTf)<sub>2</sub>], dppf = 1,1'-Bis(diphenylphosphino)ferrocene (**A8**)

*cis*-[(dppf)Pt(OTf)<sub>2</sub>], dppf = 1,1'-Bis(diphenylphosphino)ferrocene (**A9**)

[RuCl<sub>2</sub>(PPh<sub>3</sub>)<sub>3</sub>] (**A10**)

3,6-Bis[*trans*-platinum(triethylphosphine)<sub>2</sub>(nitrate)-(ethynyl)]carbazole (**A11**)

*cis*-[Pd(dppp)(O<sub>3</sub>SCF<sub>3</sub>)<sub>2</sub>], dppp = 1,3-Bis(diphenylphosphino)propane (**A12**)

*cis*-Pd(dppp)(OTf)<sub>2</sub>, dppp = 1,3-Bis(diphenylphosphino)propane (**A13a**)

*cis*-Pd(dppe)(OTf)<sub>2</sub>, dppe = 1,2-Bis(diphenylphosphino)ethane (**A13b**)

4,4',4''-Tris[ethynyl-*trans*-Pt(PEt<sub>3</sub>)<sub>2</sub>(NO<sub>3</sub>)]triphenylamine (**A14**)

### Authors' Biographies



Anurag Mishra received his B. Sc. and M. Sc. degrees from Dr. Ram Manohar Lohia Avadh University, Faizabad, India. He obtained his Ph.D. (2008) from the University of Delhi, India, under the guidance of Prof. Rajeev Gupta. He worked as a postdoctoral fellow with Prof. Gagik Melikyan at the California State University, Northridge, USA (2008-2009) and with Prof. Ki-Whan Chi at the University of Ulsan, South Korea (2010-2013). Currently, he is working as DST Fast Track scientist at the Indian Institute of Technology, Kanpur, India. His research interests are in the area of coordination-driven self-assembly, organometallic materials, and metal organic frameworks.



Rajeev Gupta obtained his PhD from the Indian Institute of Technology – Kanpur in 2000 under the supervision of Professor RN Mukherjee. He did his post-doctoral work with Professor AS Borovik at the University of Kansas during 2000 – 2003. He joined the Department of Chemistry, University of Delhi in 2003 and presently working as an Associate Professor. His research interests are in the area of bioinorganic, supramolecular, and coordination chemistry with focus on architectural aspects, functional materials and catalysis.